Ore Geology Reviews 73 (2016) 432–450

Contents lists available at ScienceDirect

Ore Geology Reviews

journal homepage: www.elsevier.com/locate/oregeorev

Geochemical exploration challenges in the regolith dominated Igarapé Bahia gold deposit, Carajás, Brazil

Claudio Gerheim Porto

Department of Geology, Federal University of Rio de Janeiro—UFRJ, Brazil

ARTICLE INFO

Article history:
Received 11 April 2015
Received in revised form 23 October 2015
Accepted 24 October 2015
Available online 29 October 2015

Keywords:
Gold
Laterite regolith
Geochemical exploration
Carajás
Brazil

ABSTRACT

The Igarapé Bahia, situated in the Carajás Mineral Province, is a world-class example of a lateritic gold deposit. It has developed under tropical weathering conditions since at least the Eocene and resulted in a regolith cover of at least 100 m thickness. The regolith is dominated by ~80 m thick ferruginous saprolite containing gossan bodies that constitute the main Au ore. Above saprolite the regolith stratigraphy has been established considering two distinct domains. One composed of residual materials and the other transported materials deposited over palaeochannels. In the residual domain the ferruginous saprolite grades upwards into a fragmental duricrust, interpreted as a collapsed zone, and then into different types of ferruginous duricrusts. Over palaeochannel the ferruginous saprolite is truncated by poorly sorted ferruginous sediment of variable composition that grades upwards into the ferruginous duricrusts formed over transported materials. Lateritization took place during a marked period that transformed the colluvium of the residual domain, and the transported materials accumulated in the channel depressions, into the ferruginous duricrust units. A later bauxitization event has overprinted all duricrust types but has mostly affected the duricrusts over the palaeochannel forming gibbsitic nodules. All duricrusts were finally covered by a transported layer of latosol which flattened the whole landscape in the Carajás region. Gold shows a depletion trend across the regolith but is enriched in the fragmental duricrust below the ferruginous duricrust from which gold is leached. Gold is also chemically dispersed laterally into the fragmental duricrust, but lateral Au dispersion in the ferruginous duricrusts of the residual domain is probably also influenced by colluvial transport. Metals associated with Au mineralization (Cu, U, Mo, Pb, Ag, LREE, Sn, W, Bi, Sb and P) are generally depleted in the saprolite but most of them are still anomalous. The fragmental and ferruginous duricrusts are more leached but the tests performed to estimate the dispersion potential of metals contained in the ferruginous duricrust show that some metals are still significantly anomalous especially Au, Ag and Cu. However, if ferruginous duricrusts are used as an exploration sample media their environment of formation must be considered. Metal depletion is generally more advanced in the ferruginous duricrusts developed in the vicinities of palaeochannels as oppose to those developed in residual domain. On the contrary, Au over palaeochannel areas is enriched in the upper bauxitized ferruginous duricrusts and in their gibbsitic nodules as a result of lateral chemical transport that is more widespread than in the colluvium over residual domain. The latosol is highly depleted in most metals due to its transported nature. However, the nodular fractions of the latosol show the greatest dispersion potential especially for Au, Ag, W, U, Bi and Sn. It can incorporate magnetic nodules that bring a rich suit of metals associated to the magnetic gossans, and non-magnetic nodules, classified as concretion and pisolites, which bring metals enriched or dispersed in the ferruginous duricrusts. This suggests that Lag constitutes a promising sample medium for geochemical exploration in the lateritic terrains of the Carajás region.

1. Introduction

The Igarapé Bahia Au mine is located in the deeply weathered Carajás mineral province where several IOCG type Cu–Au ore bodies have been discovered as a result of intense regional exploration programs conducted by Vale Ltd. since the 1970s. However, mineral exploration has been severely hampered by the presence of tropical rain forest and lack of surface exposure due to thick lateritic regolith cover.

The first indication of Cu mineralization at Igarapé Bahia was detected from regional stream sediment geochemical surveys. However, due to the development of extensive lateritic plateaus covered by highly leached latosols, follow-up soil geochemistry surveys failed to identify the ore body, until it was realized that dispersed gossan fragments in the latosol were the only signs of mineralization at the surface (Costa et al., 1996). This, coupled with the aid of magnetometric surveys, delineated the target, which nonetheless proved to be economic only for Au in the regolith. According to Tallarico et al. (2005) the primary sulfide Cu–Au resource is estimated at 219 Mt @ 1.4% Cu and 0.86 g/t

E-mail address: porto@geologia.ufrj.br.

http://dx.doi.org/10.1016/j.oregeorev.2015.10.027
0169-1368/

Au but remains sub-economic to date. The bulk of the gold was mined from the regolith for nearly 10 years until 2002 when the open pit reached bedrock or saprock at a depth of about 100 m. The original regolith ore reserves were 30 Mt @ 3.2 g Au/t.

The aim of this work is to establish the regolith stratigraphy of the deposit and discuss the origin of the regolith units and their relations to the geochemical features observed and suggest how this can be applied to improve geochemical exploration procedures in the lateritic terrains of the Carajás province. The results of this work are based on research conducted as part of the LATAM Project (Porto, 2007).

2. Geology of the deposit area

The Igarapé Bahia Au mine is associated with a volcano–sedimentary sequence which is part of the Late Archaean (c. 2.75 Ga) Itacaiunas Supergroup metamorphosed to upper greenschist to amphibolite grade (Docegeo, 1988; Fig. 1). The sequence is covered by platformal sedimentary rocks of the Águas Claras Formation (Nogueira et al., 1994) which is intruded by Late Archaean to Proterozoic granites (Barros et al., 2004; Tallarico et al., 2004). Sills and dykes of quartz–diorite and gabbro dated at 2.67 Ga (Nogueira et al., 1994), controlled by fractures and normal faults, cut both the Itacaiúnas and the Aguas Claras Formations. The rocks of the Igarapé Bahia sequence are exposed in a tectonic and erosional window of the Aguas Claras Formation. Primary ore is confined to a hydrothermal breccia layer situated at the contact between a lower unit, composed of mafic volcanic rocks and iron formations, and an upper unit, formed mostly of sedimentary rocks. The ore occurs in three main bodies arranged in a semi-circular feature which dips steeply away from a mafic volcanic dome in the centre (Fig. 2).

The mineralized breccia is composed of host rock fragments and a matrix containing disseminated to locally massive, fine-grained chalcopyrite with associated magnetite, gold, and other minor sulfides including bornite, cobaltite, molybdenite, digenite and pyrite. Mineralization is also found disseminated in some brecciated footwall mafic volcanic rocks, as well as in brecciated parts of the sandstone succession close to the main ore zone (Dreher et al., 2008). Hydrothermal alteration in the breccia zone and host rocks is characterized mainly by the presence of sulfides, chlorite, magnetite and siderite (Dreher et al., 2005; Tallarico et al., 2000). Monazite has also been identified as an alteration product in the breccia ore and it has been dated to 2575 ± 12 Ma, which characterizes the mineralization as epigenetic (Tallarico et al., 2005). Gold is found as 5–20 μm particles included in gangue and ore minerals. Individual grains may contain up to 12% Ag, and inclusions of silver tellurides or sulfides (Tallarico et al., 2000).

The main metals accompanying Cu–Au mineralization in the primary ore are U–Mo–Pb–Sn–Ag–Bi–Sb–W–P–rare earth elements (REE) (Tallarico et al., 2005; Tavaza and Oliveira, 2000; Almada and Villas, 1999). This assemblage forms the basis for further geochemical investigation in the regolith as part of this work.

3. Geomorphology and regolith geology

The Carajás region is dominated by extensive lateritic plateaus with elevations ranging from 750 to 900 m. These are being eroded by the present drainage network resulting in surrounding lowland areas with elevations of 250 to 350 m. The plateaus are capped by ferruginous duricrust (Eggleton, 2001) overlain by latosol (Ker, 1997).

Ar/Ar dating of Mn oxides from the duricrust yields ages as old as 70 Ma, but most concentrate around 50 Ma (Vasconcelos et al., 1994). This indicates that the peak of duricrust formation took place in the Lower Eocene.

At Igarapé Bahia the regolith thickness may reach 150 m over the ore zone, and it has been described as a gossan profile by Costa et al. (1996). The regolith profile is marked at its base by a transition zone, up to 50 m thick, between protolith and saprolite. The Cu minerals present are native Cu, chalcocite, malachite, and azurite. Above this is the oxide ore zone that is nearly 100 m thick. It is dominated by a ferruginous saprolite containing gossan zones over the hydrothermal breccia. The ore comprises resistate magnetite bodies intermixed with iron oxyhydroxide and clay alteration products derived from hydrothermal breccia. This ore is termed magnetite gossan in this work, but disseminated Au also occurs in ferruginous saprolite over hydrothermally altered and brecciated mafic volcanic and sedimentary rocks close to the gossan ore zone. Above the saprolite is a complex zone dominated by duricrusts. This zone is described by Costa et al. (1996) as a lateritic crust, and Costa (1997) and Costa et al. (1993) recognized a bauxitic horizon in its lower portion. In the mine nomenclature, this zone is termed a mixed zone, which forms a mushroom-shaped disseminated ore covered by a barren latosol layer with which it is in sharp contact.

This latosol layer is commonly found on top of ferruginous and aluminous duricrust in the Amazon, but its origin is debatable. It was first described by Sombroek (1966) who named it “Belterra Clay” after its type locality, but it has been identified in several other locations in the Amazon. Some authors claim that it is formed in situ as a result of

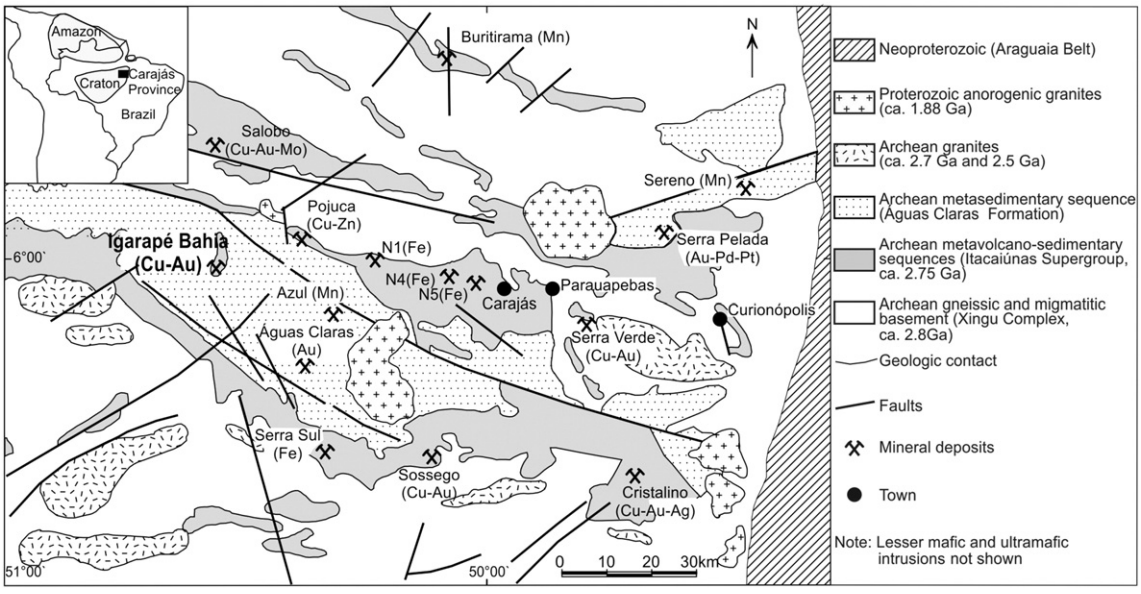

Fig. 1. Geological map of the Carajás Mineral Province with location of Igarapé–Bahia and other important deposits. Based on Docegeo (1988) and Tallarico et al. (2000).

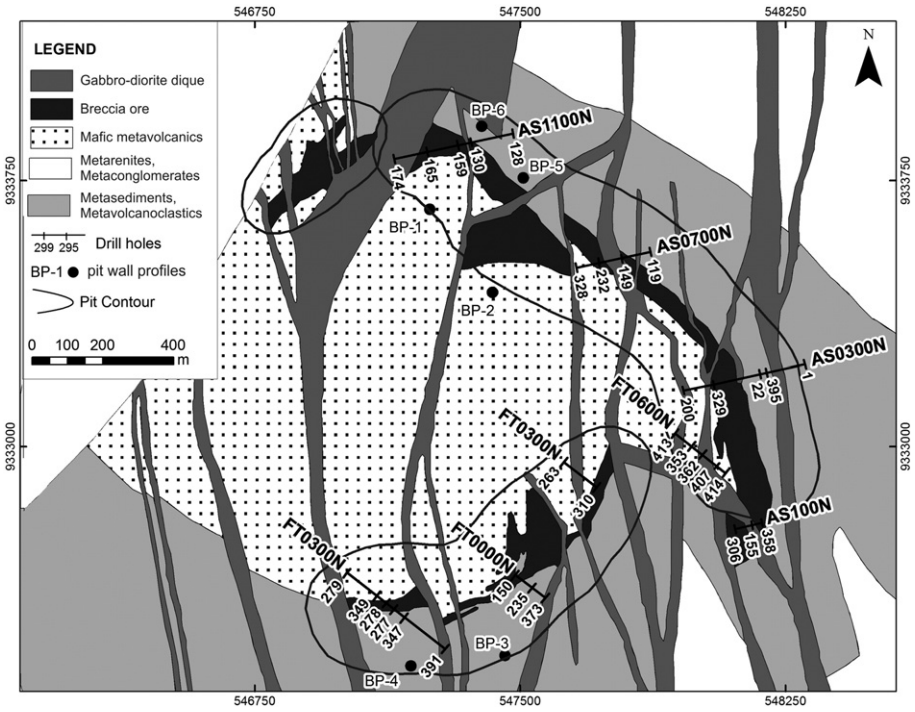

Fig. 2. Geological map of the Igarapé Bahia deposit area showing the three main pits plus the location of diamond drill holes and pit wall profiles studied. Modified from Tallarico et al. (2000).

physical and chemical breakdown of the ferruginous duricrust (Horbe and Costa, 2005; Boulangé et al., 1997; Leprun, 1979; Beauvais and Tardy, 1993; Lucas et al., 1989) while others thought that it represents either mass flow deposits generated under arid conditions (Hieronymus et al., 1989; Truckenbrodt and Kotschoubey, 1981; Grubb, 1979) or a highly leached Quaternary sediment (Kronberg et al., 1982). This latosol layer, duricrusts and ferruginous zones of the regolith are the focus of this work.

4. Methodology

The regolith stratigraphy was established by an extensive survey in the pit areas followed by detailed logging of diamond drill core. Pit wall sections were mapped in detail with GPS control. Pit benches were used for vertical reference and the contacts along the pit walls were determined using a measuring tape. This survey concentrated on the uppermost 20 m pit benches in order to characterize regolith units above the saprolite. About 800 m of pit wall sections were surveyed in this way. Six vertical channels, each approximately 20 m long, were excavated in selected pit walls and described and sampled in detail. This was complemented by logging and sampling 33 diamond drill holes. Most of these drill holes reached a depth of around 50 to 60 m Gold and Cu grades from those drill cores were utilized to study grade distribution across the regolith, with lower levels of detection for Au of 0.01 ppm and Cu 0.01%. Eighteen of these drill holes had magnetic susceptibility measured at meter intervals using a portable magnetometer (Exploranium KT-9). These data constitute the exploration database with about 2500 core samples.

Another set of samples were analyzed for multi-element. They constitute the drill hole core samples comprising the composite section AS1100N that crosscuts the mineralized zone, plus 2 drill holes core samples in the protolith. Multi-element analysis also includes all pit wall channel samples collected away from the ore zone which has been mostly mined out at the time of sampling. Nearly two hundred channel and core samples, 2 to 3 kg each were analyzed for multi-element.

Samples were divided into two domains, one representing the ore zone, and the other the dispersion zone. Those samples representing the dispersion zone are situated 50 m to 200 m laterally adjacent to the ore zone, and typically intersected barren, or very low-grade, Au zones in the saprolite. The location of all channels and diamond drill holes are shown in Fig. 2.

Multi-element geochemical analyses were done by ACME Laboratories. For SiO_2, Al_2O_3, Fe_2O_3, CaO, MgO, Na_2O, K_2O, MnO, TiO_2, P_2O_5, Cr_2O_3 and Sc the samples were fused with $LiBO_2$, digested with nitric acid and analyzed by ICP-AES. For REE, Ba, Be, Co, Cs, Ga, Hf, Nb, Rb, Sn, Sr, Ta, Th, U, V, W, and Zr, the samples were fused with $LiBO_2$, digested with nitric acid and analyzed by ICP-MS. For Ag, As, Au, Bi, Cd, Cu, Hg, Mo, Ni, Pb, Sb, Se, Tl, and Zn, each sample was digested using aqua regia, and concentrations measured by ICP-MS. Au was analyzed on 30 g pulps by fire assay after bead dissolution in aqua regia and ICP-ES finish with a detection limit of 2 ppb. Ten examples of analytical results are displayed in the Appendix A.

Undeformed channel samples from the BP-1 and BP-2 pit wall profiles were examined petrographically, and using an SEM fitted with secondary and backscatter electron detectors and an EDS microanalyser (Link ISIS L300). X-ray diffraction semi-quantitative analysis of sample powder was conducted using a PHILIPS model PW 3710 diffractometer.

5. Stratigraphy of the regolith

Based on the description of pit walls, drill hole cores and channel sampling, eight regolith units could be the identified. Importantly, palaeochannels were identified in at least three different localities in the pit walls. These are represented by the channel samples from the BP-1 and BP-3 and BP-5 profiles, located in the dispersion zone. At these localities the saprolite is found below an erosive contact with the overlying ferruginous zones and duricrusts that represent a transported cover. In this work this is considered the transported domain. The other localities studied are in the residual domain, either over the ore zone or dispersion zone, although the latosol layer ubiquitously present covering all regolith units is always transported. The regolith stratigraphy is schematically displayed in Fig. 3. However

it should be emphasized that over the ore zone the different types of ferruginous duricrust are not easily differentiated in drill cores as the regolith is dominated by gossan bodies that show a more general nodular structure. For that reason the regolith stratigraphy has been simplified over the ore zone to allow comparisons between the geochemical features of the ore and dispersion zones. In these cases only 4 regolith units are considered: saprolite; fragmental duricrust; ferruginous duricrust; and latosol.

Saprolite is invariably ferruginous, clay-rich and quartz-poor. Over the hydrothermal breccia, it hosts Au ore, most of which is associated with the magnetite gossans. Saprolite over siltstones is richer in quartz and more mottled, whereas saprolite over diorite and gabbro dikes is richer in kaolinite (Fig. 4A).

In the residual domain the saprolite grades upward into a fragmental duricrust (Eggleton, 2001) up to 5 m thick (Fig. 4B). The fragments range in size from a few centimeters to one meter blocks of ferruginous duricrust and ferruginous saprolite all set in a Fe- and clay-rich matrix. Fragments of iron formation and magnetite bodies are also common where these occur in the underlying ferruginous saprolite. These features suggest that it represents a collapsed zone developed basically in situ.

Over the palaeochannel the saprolite is in sharp contact with more friable and diversified regolith materials. It may show some sedimentary features as observed at the base of the palaeochannel in the BP-3 pit wall profile where a type of sedimentary breccia, with similar features to a ferricrete (Eggleton, 2001), occurs truncating a gabbro dike saprolite (Fig. 4C). It is composed of angular fragments of iron formation cemented by a ferruginous matrix. Similarly, at the base of the palaeochannel in the BP-1 pit wall profile, the saprolite is in sharp contact with a zone containing different types of granular fragments set in a ferruginous clay matrix suggesting it is a transported cover. This zone has been collectively termed ferruginous sediments (Fig. 3).

There is a lateral transition between the fragmental duricrust, developed in the residual domain and the transported ferruginous sediments whose material have probably derived from the erosion of the upper portions of the saprolite prior to its lateritization.

The upper part of the section contains the ferruginous duricrusts which may reach up to 7 m thick. The dominant type is a purple duricrust which contains irregular shaped ferruginous nodules up to 1 cm cemented in a highly ferruginous fine-grained matrix. Yellow duricrust is usually found above the purple duricrust but also as irregular masses and semi-vertical lobes penetrating into the lower purple crust sometimes reaching the fragmental duricrust (Fig. 4G). It contains more abundant ferruginous nodules, regular in shape and with smoother surfaces. These features suggest that it results from past biogenic action such as root penetration that took place before lithification of the duricrust. Although there are no macroscopic distinguishing features between the purple or yellow duricrusts over the palaeochannel areas and the residual domain, it must be considered that any material above the ferruginous sediments over palaeochannels must be transported. The similarity between the purple or yellow duricrusts of the transported and residual domains may be due to lack of sorting during transport and homogenization as a result of subsequent lateritization.

The ochre duricrust is found only over palaeochannel areas in sharp contact with the latosol. It is generally more friable and made up of irregular yellow nodules set in fine-grained ferruginous matrix (Fig. 4E). It grades laterally into the yellow and massive duricrusts over distances of up to one hundred meters away from palaeochannels. The massive duricrust is purple-red, has a pisolitic and highly cemented fabric (Fig. 4F) and occurs only in the residual domain probably representing paleo-high relief areas.

The latosol layer at the top of the regolith profile is always in sharp contact with the underlying duricrust units. Over the palaeochannel areas, its thickness may reach 20 m, but in the residual domain it varies from 1 to 6 m (Fig. 3). The latosol has an orange color and contains ferruginous nodules up to 0.5 cm that are both sparsely disseminated, but more commonly found concentrated at the base. Ferruginous nodules separated from the coarse fraction (>0.5 mm) of the latosol fall into three categories. One type is non-magnetic and consists of well-rounded, smooth pisolites (Fig. 4D). The second type is also non-magnetic, nodules have irregular shapes and rough surfaces and were termed concretions (Fig. 4H). The third type, separated with a hand magnet, is similar in appearance to concretions. These nodules form a surface lag, similar to those observed in Western Australia where they proved to be an effective sampling medium for geochemical exploration (Cornelius et al., 2001; Anand and Butt, 2010; Anand and Paine, 2002; Anand, 2001).

The regolith stratigraphy for section AS1100N in the residual domain was constructed from drill hole data as shown in Fig. 5. It shows that the latosol layer is much thinner over the ore zone where the magnetite gossans probably formed an area of higher relief in the paleotopography. The latosol becomes thicker laterally away into the dispersion zone, and even thicker over palaeochannel areas (not

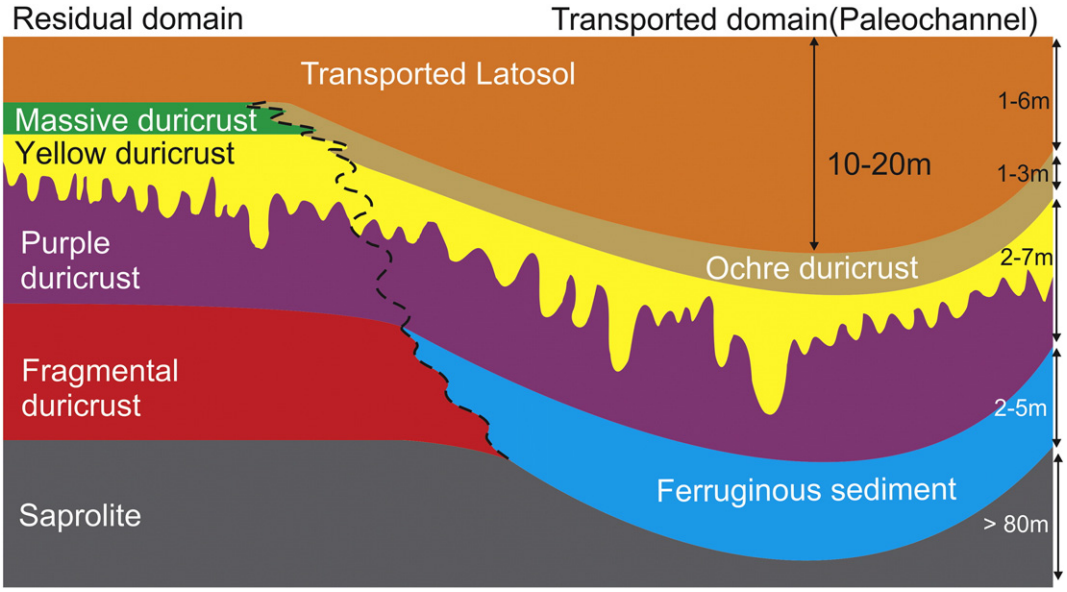

Fig. 3. Schematic representation of the regolith stratigraphy of the Igarapé Bahia area. Dashed line separates transported (towards palaeochannel) from residual domains.

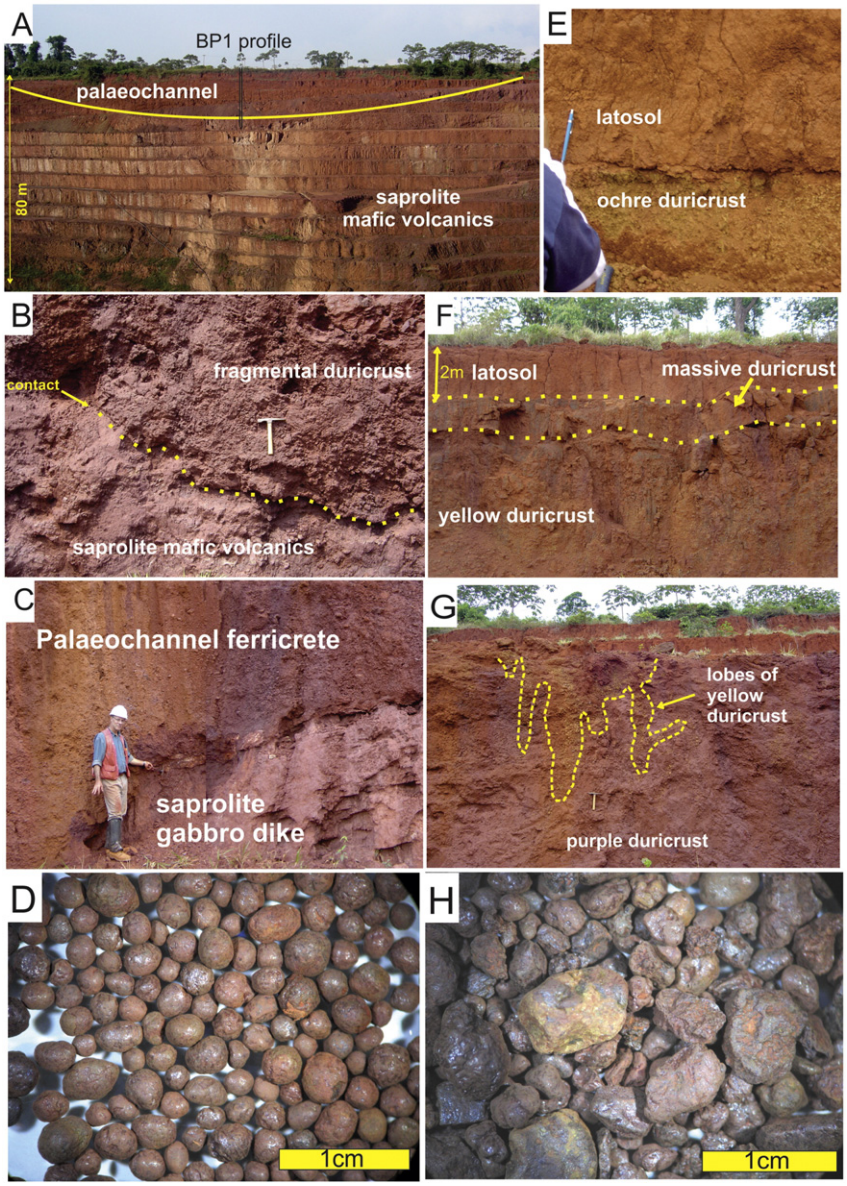

Fig. 4. Macroscopic features of the regolith units: A) View of the ferruginous saprolite truncated by palaeochannel showing the location of the BP-1 pit wall profile. B) Irregular contact of saprolite and fragmental duricrust (hammer is 30 cm). C) Erosive contact between saprolite and base of palaeochannel filled with sedimentary breccia (ferricrete). D) Smooth pisolitic nodules extracted from the latosol. E) Sharp contact between ochre duricrust and latosol over palaeochannel areas. F) Yellow duricrust overlain by massive duricrust with latosol layer on top. G) Vertical lobes of yellow duricrust penetrating into the purple duricrust. H) Irregular Fe-concretions extracted from the latosol.

shown in the Fig. 5). Thus, the latosol represents an original clay-rich material that was deposited over previously-formed duricrust, and its source constituted areas of higher relief in the paleo-topography, including the nearby ore zone. This is in contrast to the work of Horbe and Costa (2005) who suggested that it was a product of the degradation of ferruginous duricrust.

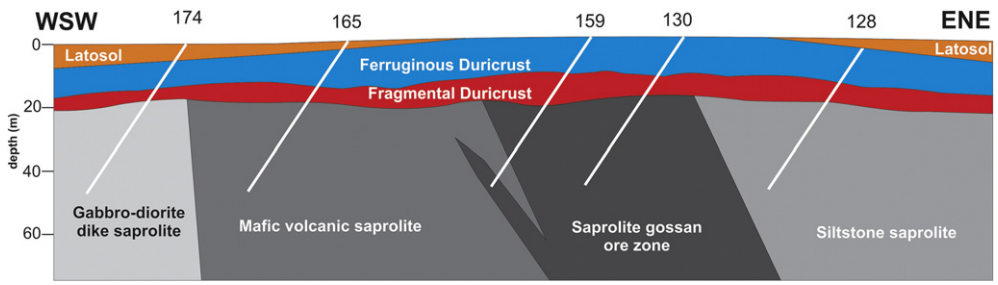

Fig. 5. Section AS1100N across the mineralized zone showing saprolite and duricrust overlain by latosol layer. Note over gossan zone latosol is absent.

6. Mineralogy and micromorphology of the regolith

Semi-quantitative XRD analysis coupled with the results of whole-rock chemistry, show that the main minerals present in the regolith are hematite, goethite, gibbsite and kaolinite. Their relative abundances are as shown in Fig. 6 for profile BP1 over a palaeochannel, and for BP-2, in the residual domain over the dispersion zone.

The saprolite is distinctly kaolinite rich. Micromorphological analysis under the SEM shows that it is characterized by the presence of "kaolinite booklets" composed of intermixed laminae of kaolinite and Fe oxides that are pseudomorphs after primary chlorite (Fig. 7A). Over palaeochannel (i.e. BP-1 profile) kaolinite quickly diminishes upwards into the ferruginous sediments and all ferruginous duricrust above where gibbsite is most abundant. In the residual domain (i.e. BP-2 profile) kaolinite also diminishes upward into the fragmental and ferruginous duricrusts above, but to a lesser degree, and gibbsite is less abundant compared to the BP-1 profile.

In the BP1 profile the purple duricrust shows a gibbsitic matrix and the saprolite fabric, such as "kaolinite booklets" is not preserved, but the ferruginous nodules are intensely fractured and filled by gibbsite

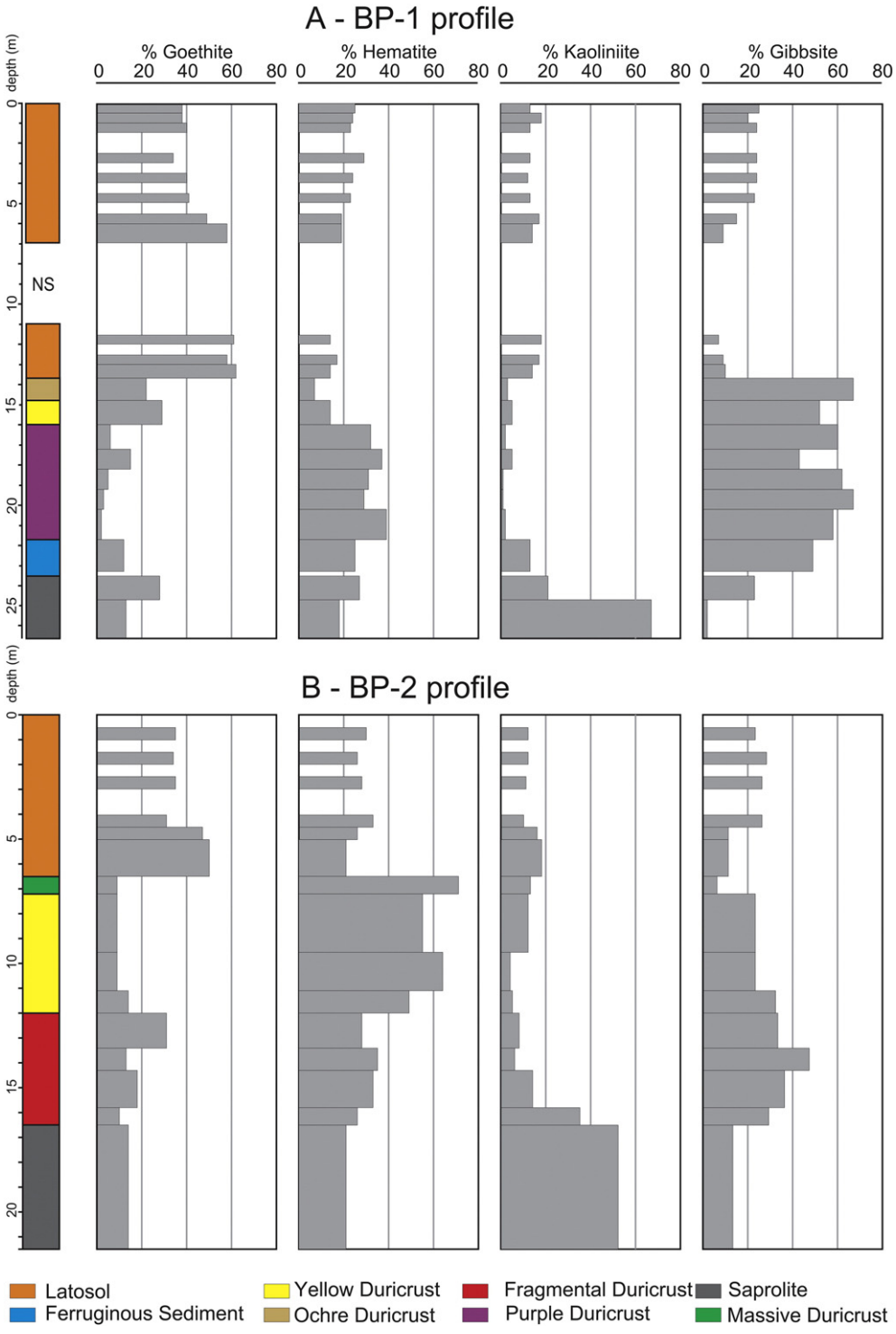

Fig. 6. Semi-quantitative XRD analysis of BP-1 profile over palaeochannel and BP-2 profile in the residual domain away from palaeochannel (NS — not sampled) (after Corrêa Neto, 2009).

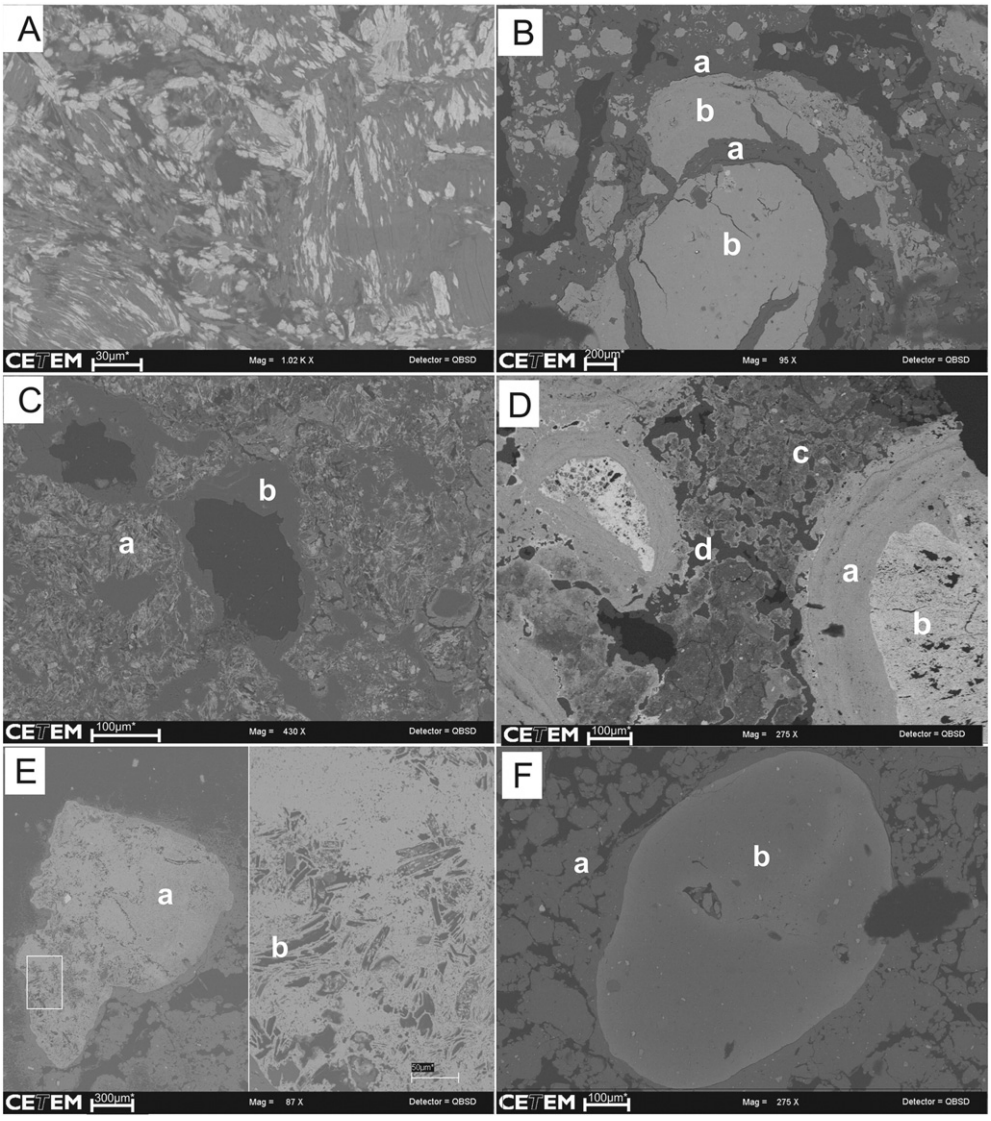

Fig. 7. Scanning electron microscope photomicrographs (backscattered images) of the regolith units: A) Sample BP2 — 20 m — saprolite: "booklets" of kaolinite laminae (gray shades) intermixed with Fe-oxides (in white) as pseudomorphic replacement after chlorite. B) Sample BP1 — 19 m — purple duricrust: a) gibsite filling fractured Fe-nodule and in the matrix; b) Fe-nodule. C) Sample BP2 — 14 m — fragmental duricrust: a) kaolinite "booklets"; b) gibbsite lining voids. D) Sample BP2 — 8 m — yellow duricrust: a) córtex of goethite–kaolinite; b) hematitic core; c) kaolinite matrix; d) gibbsite lining voids in the matrix. E) Sample BP-1 — 6 m — latosol: Fe-concretion: a) Fe-oxide; b) detail showing relicts of kaolinite "booklets". F) Sample BP-1 — 1–6 m — latosol: pisolite with smooth contours: a) Fe-kaolinite of the latosol matrix; b) Fe-kaolinite nodules (after Corrêa Neto, 2009).

(Fig. 7B). This contrasts with the BP2 profile where the fragmental and ferruginous duricrusts contain relicts of saprolite fabric (Fig. 7C), but the ferruginous nodules are not fractured and gibbsite concentrates only in the matrix (Fig. 7D).

The yellow and ochre duricrust units in BP-1 profile are rich in goethite and gibbsite compared to the top yellow and massive duricrust units found in BP-2 profile which is richer in hematite (Fig. 6). These features show that the "bauxitization" event that has overprinted the duricrust units was much stronger in the BP-1 profile, and has completely obliterated the saprolite fabric, which suggests more intense leaching and hydration occurred over the palaeochannel.

The latosol layer in BP1 is more kaolinitic than the underlying ferruginous duricrusts. It is richer in gibbsite and poorer in goethite towards the surface, which may reflect post-depositional alteration. There is a clear break in composition between the ferruginous duricrust and the transported latosol layer. Micromorphological analysis of the ferruginous nodules from the latosol shows that the concretion nodules have relicts of "kaolinite booklets" (Fig. 7E). This is true also for the concretion nodules collected over the palaeochannels where duricrust units lack these relicts. This implies that these concretions were derived from upslope, and have been deposited with the latosol layer filling the palaeochannel depressions where the duricrusts are more gibbsitic and lack relicts of "kaolinite booklets". The pisolites show a more homogeneous texture and composition (Fig. 7F), and are largely composed of a ferruginous kaolinitic material, similar to the soil matrix in which they are found. Pisolites with similar features have been described in some palaeochannels of Western Australia, and were interpreted as forming in situ (Thorne et al., 2014; Anand and Verrall, 2011).

7. Major element geochemistry of the regolith

The geochemical composition of the regolith units has been evaluated using ternary plots Si–Al–Fe. Other major elements add up to less than 3% and are not discussed here. The Si/Al ratio for kaolinite is also shown in the ternary plots (Fig. 8A and B). Samples containing gibbsite will show a lower Si/Al ratio. In these plots the samples from the purple and yellow duricrusts located over palaeochannel are separately marked.

Iron is enriched from saprolite upwards reaching a maximum in the massive crust which is more hematitic (Fig. 8A) but also the most

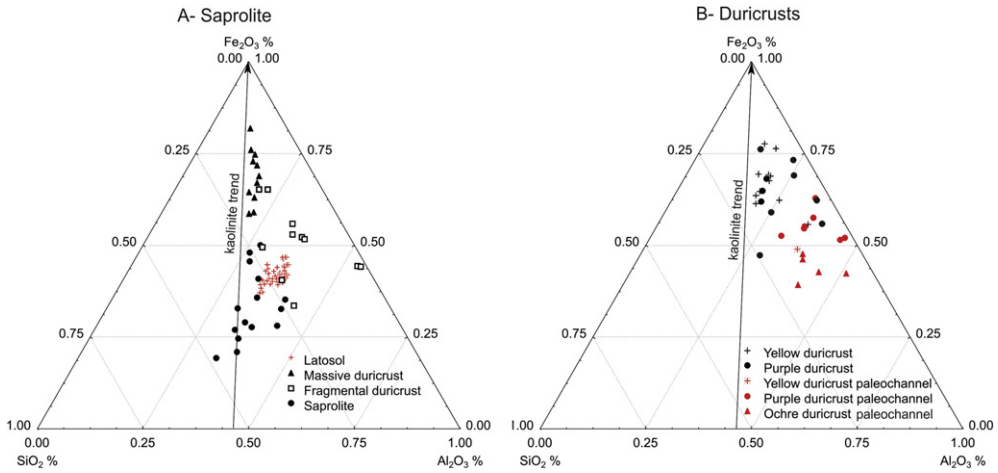

Fig. 8. Ternary plots for Si–Al–Fe. A — Saprolite; fragmental duricrust; massive duricrust and latosol. B — Purple, yellow and ochre duricrusts. Palaeochannel samples highlighted in red.

kaolinitic type of duricrust. Its massive nature prevents stronger leaching and gibbsite formation after lateritization. The ochre duricrust and latosol are similarly Fe poor. Above saprolite the fragmental duricrust acquires a more gibbsitic composition and this trend continues into the purple and yellow duricrusts. The palaeochannel samples from the purple and yellow duricrusts are less ferruginous and more gibbsitic compared to the corresponding samples in the residual domain (Fig. 8B). The samples from the ochre duricrust, over palaeochannel, are distinctly gibbsitic. The composition of the latosol is more homogenous and more kaolinitic although gibbsite is also present. These observations are in accordance with the XRD and SEM data presented above. The data indicate that bauxitization of the duricrusts over palaeochannel, specially the ochre duricrust, is stronger.

8. Relationships between gold and copper grades and magnetic susceptibility

Results of magnetic susceptibility measurements on drill core coupled with the corresponding Au and Cu grades obtained from the drill hole exploration database are plotted in Fig. 9. The plots show each sample in the x-axis arranged in terms of decreasing Au grades, separately in the ore zone and dispersion zone, across the regolith.

In the protolith (Fig. 9A) the higher Au grade samples are generally accompanied by magnetite- and Cu-rich samples, although there is no direct correlation between magnetite or Cu and Au. Magnetite, Cu and Au are virtually absent in the dispersion zone.

A similar relation between Au and magnetite is observed in the saprolite (Fig. 9B), where the higher Au grade samples are generally accompanied by magnetite-rich samples from the gossan zones. However, the Cu grades are invariably low and there is little difference between the ore and dispersion zones.

In the fragmental duricrust (Fig. 9C) the higher Au grade samples of the ore zone become independent of the magnetite gossan samples. Furthermore, in the dispersion zone magnetite-rich samples are absent, but there is a group of samples with Au grades as high as nearly 2 ppm. This implies that some lateral Au dispersion has occurred although there is not lateral mechanical dispersion of magnetite gossan fragments despite collapsing.

In the ferruginous duricrust unit (Fig. 9D) the higher Au grade samples of the ore zone remain independent of the magnetite gossan samples. However, the dispersion zone contains a few magnetite-rich samples as a result of lateral mechanical dispersion showing that unlike the fragmental duricrust zone, this zone shows some degree of transport. The dispersion zone also contains samples with higher Au concentrations denoting some lateral Au dispersion as in the fragmental duricrust.

In the latosol (Fig. 9E) the magnetic susceptibility values are similar in the ore and dispersion zones, and completely independent of the Au grades, reflecting an allochthonous origin for latosol.

9. Distribution of gold and copper in the regolith

The distribution of Au and Cu using the exploration database are shown using box-plots (Fig. 10A and B) for both the ore and dispersion zones across the regolith profile.

9.1. Gold distribution

In the ore zone, the median Au grade of the protolith throughout the whole ore zone including the hydrothermal breccia, is 1.08 ppm. The median Au grades in the saprolite range from 0.46 to 1.00 ppm from 30 m to >60 m from the surface. This pattern shows that Au must have been leached during the transition from the protolith to the saprolite since there is no Au grade increase as a result of a simple density decrease in the saprolite. In the upper 10 m of the saprolite there is substantial grade increase to 2.45 ppm. In the fragmental duricrust the median Au grade reaches a maximum of 3.24 ppm. The enrichment pattern observed in the upper parts of the saprolite and fragmental duricrust could be interpreted as purely residual due to increased leaching of the saprolite and collapse of the fragmental duricrust. However, the lack of relation between the higher Au grade samples and magnetic gossans in the fragmental duricrust (Fig. 9C) suggests that Au has been mobilized from the gossans and is not, therefore, purely residual. Gold enrichment in the fragmental duricrust is probably influenced by chemical reprecipitation of the Au leached from the ferruginous duricrust, where the median Au grade drops sharply to 1.34 ppm. Gold leaching from ferruginous duricrusts has been discussed by Freyssinet (1993) as a common process in humid tropical laterites of West Africa where sub-micron sized Au particles are found re-precipitated in the mottled zone below a Au-leached iron-rich duricrust. Despite evidence of chemical leaching of Au from the ferruginous duricrust, the addition of barren material to this unit as a result of transport may also have resulted in dilution of Au grades.

Over the dispersion zone, the median Au grade of the protolith is 0.1 ppm and across the saprolite it varies from around DL (0.05 ppm) to 0.25 ppm and includes some mineralized intervals as shown by some high-grade samples. The similar Au grades of the protolith and saprolite suggest that Au has been leached from the saprolite, as observed over the ore zone. Above saprolite there is a sharp increase in

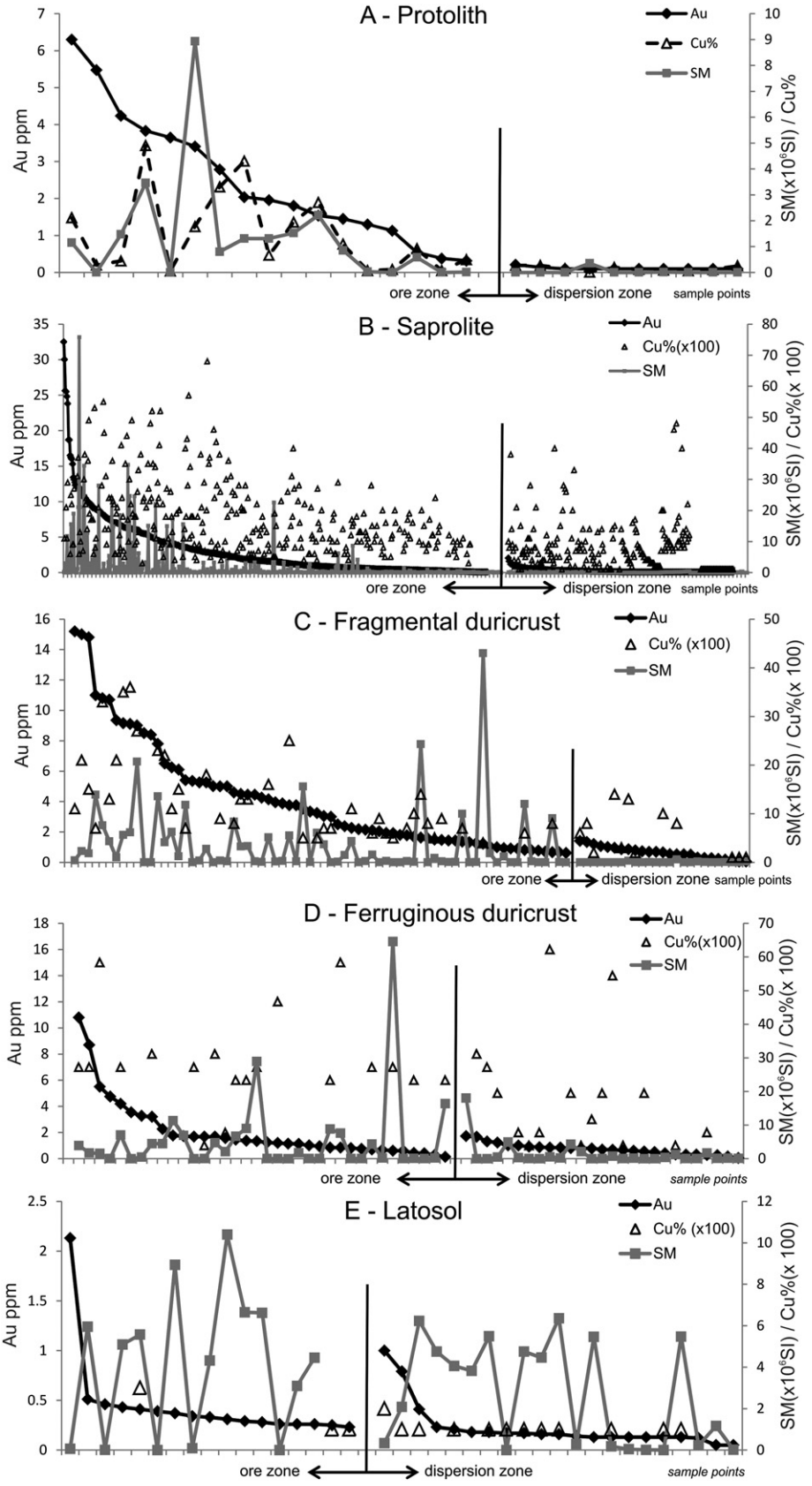

Fig. 9. Distribution of Au, Cu and magnetic susceptibility values across the regolith. For each regolith unit individual sample points are plotted in the X-axis classified by decreasing Au grades, separately in the ore zone and dispersion zone. Equivalent grades of Cu and values of magnetic susceptibility (SM) are also plotted. Copper grades are not available for all samples.

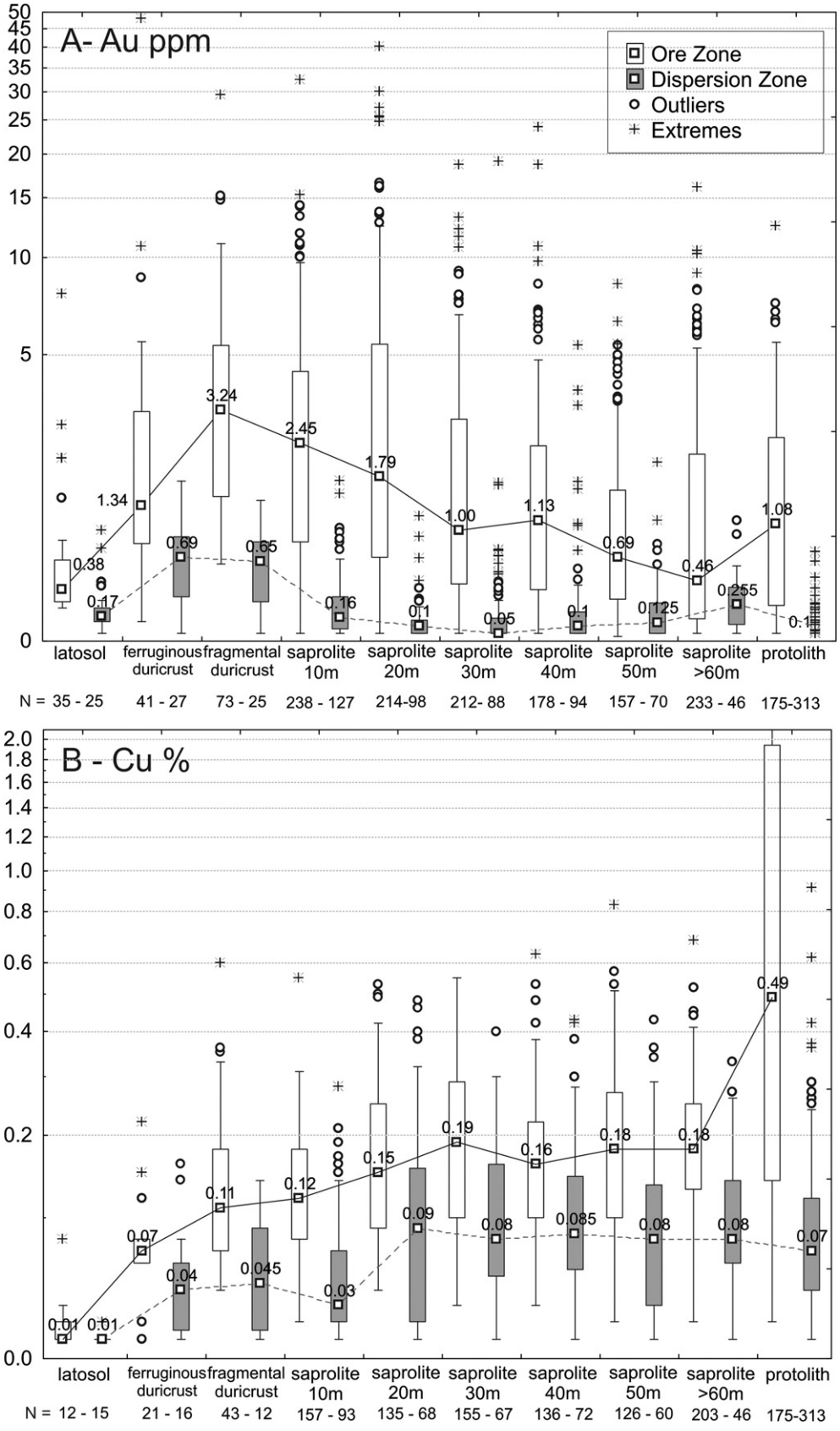

Fig. 10. Box-plots of Au and Cu grades across the regolith over the ore zone and dispersion zone. Grades in the saprolite were compiled at each 10 m depth. N indicates the number of samples in each data set.

grade in the fragmental duricrust (0.65 ppm) and ferruginous duricrust (0.69 ppm). This enrichment is in excess of that observed over the ore zone and probably results from lateral Au transport from the ore zone into the fragmental duricrust and ferruginous duricrust of the dispersion zone. In the fragmental duricrust this transport is probably mostly chemical since there is no indication of mechanical transport; however, the enrichment of Au in the ferruginous duricrust is possibly contributed by colluvium transport from the ore zone. It is also possible that part of this enrichment is directly derived from the Au enriched fragmental duricrust below as the regolith evolved downward.

In the latosol the median Au grade over the ore zone is 0.38 ppm, and in the dispersion halo it is 0.17 ppm. The low Au grade of the latosol reflects its transported nature, but the grade difference between the ore and dispersion zones is still significant.

9.2. Copper distribution

The distribution of Cu is markedly different to that of Au (Fig. 10B). In the protolith, the sulfide breccia over the ore zone shows median grades near 0.5% Cu. In the saprolite, Cu is severely leached and the median Cu grades drop to 0.12% in the upper portions of the saprolite reaching 0.1% and 0.07% in the fragmental and ferruginous duricrusts, respectively. In the dispersion zone, the Cu grade of the protolith (0.07%) remains basically unchanged across most of the saprolite. Leaching is stronger in the upper saprolite, fragmental and ferruginous duricrusts where the grades drop to 0.03%, 0.045% and 0.040%, respectively. The more severe Cu leaching over the ore zone shows that Cu is poorly retained in the gossans as opposed to the dispersion halo where most of the Cu is hosted in non-sulfide minerals, and is only slightly retained in the fragmental and ferruginous duricrusts. In the latosol over the ore and dispersion zones the Cu grades are mostly below detection limit resulting in a complete lack of contrast.

10. Geochemistry of duricrust components

To further investigate the distribution of the metals related to mineralization in all types of duricrusts present in the palaeochannel and residual domains, the multi-element data base was used considering only the samples from the dispersion zone. The results are shown in the variability plots of Fig. 11 where the samples located over palaeochannel are marked despite there being only one sample of yellow duricrust representing the palaeochannel domain.

It can be noted that most metals show a lower concentration in the ochre duricrust and in the gibbsitic purple and yellow duricrusts samples from the palaeochannel domain compared to all other types of duricrust units from the residual domain. This is the case for U, Mo, Ag, Pb, Sb, P, and Cu, shown for Cu, U, Mo and Ag in Fig. 11A, B, C and D. Other metals such as Sn, W and LREE (shown in Fig. 11E for Sn) show concentrations in the ochre, purple or yellow duricrusts from the palaeochannel domain that are not significantly different compared to all other types of duricrusts from the residual domain. A similar trend is observed for most metals considered immobile such as Ti and Zr, suggesting that these elements are residually concentrated in the duricrust units from the palaeochannel areas that suffered more intense leaching for the other metals.

Gold results are more difficult to interpret due to the relatively small number of samples analyzed in each regolith unit. However, if an attempt is made to compare the distribution of Au in the different types of duricrust (Fig. 11F), it becomes apparent that Au in the palaeochannel samples is not leached, on the contrary its distribution is closer to the immobile metals residually enriched mentioned above.

The distribution of the Au is additionally verified by in BP-1 and BP-3 profiles, over palaeochannel areas (Fig. 12). It illustrates the enrichment tendency of Au in the ochre and yellow duricrusts, and upper portions of the purple duricrust where the Au grades may reach more than 1 ppm over barren regolith. It can also be noted that this enrichment is not

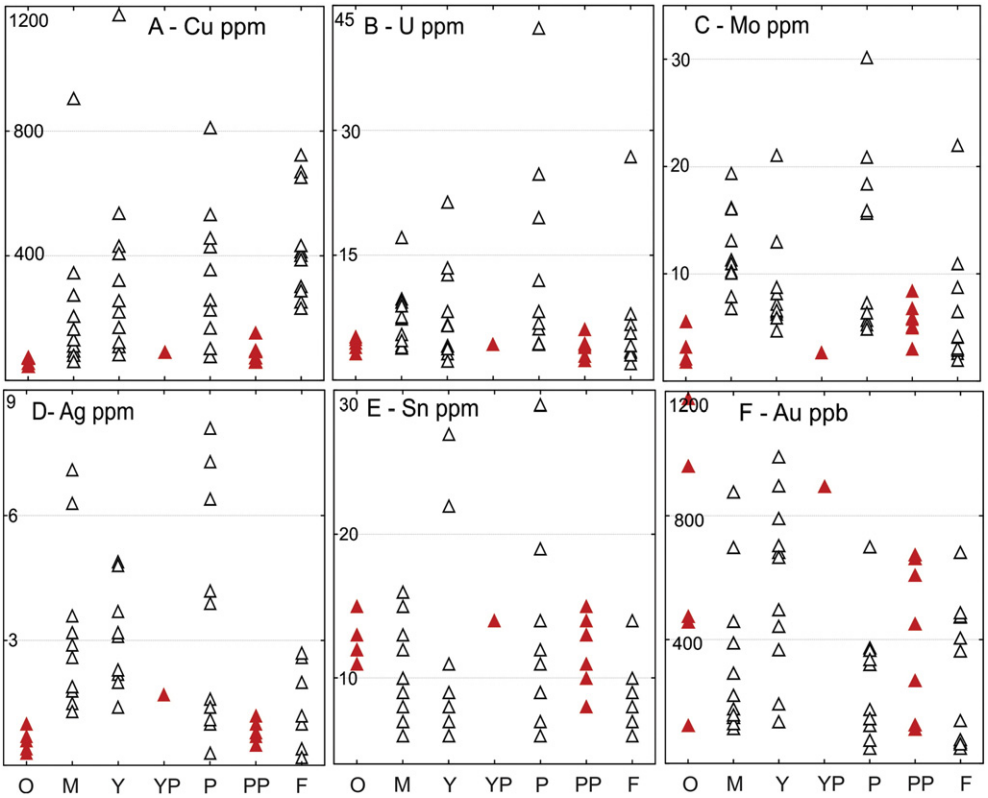

Fig. 11. Variability plots of metal concentration in the different types of duricrusts. A) Cu; B) U; C) Mo; D) Ag; E) Sn; E) Au. Palaeochannel samples marked in red. Abbreviation of regolith units: O — Ochre duricrust; M — Massive duricrust; Y — Yellow duricrust; YP — Yellow duricrust in palaeochannel; P — Purple duricrust; PP — Purple duricrust in palaeochannel; F — Fragmental duricrust.

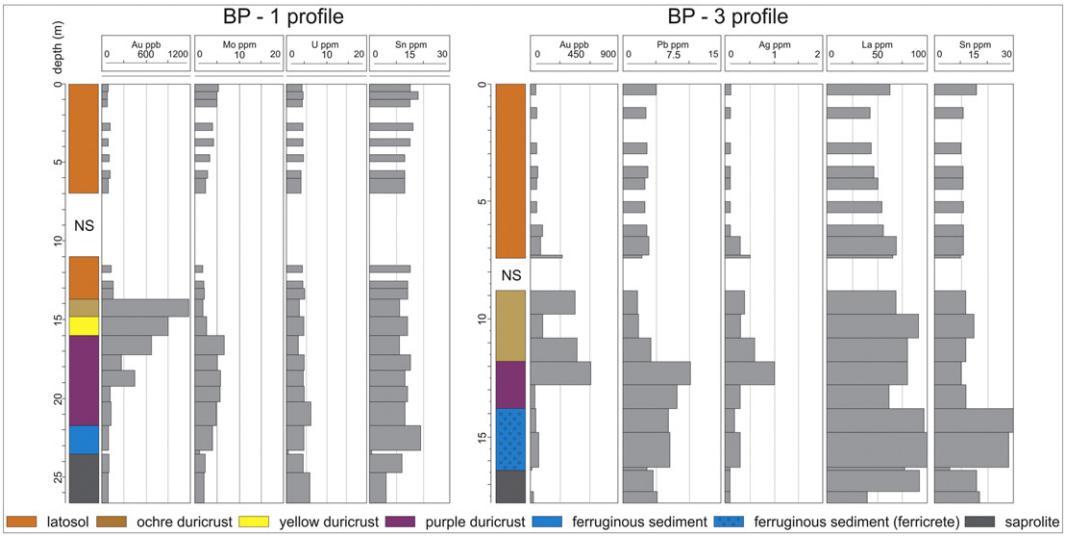

Fig. 12. Geochemical profiles BP-1 and BP-3 over palaeochannel areas showing the distribution of Au, Mo, U, and Sn for BP-1 and Au, Pb, Ag, and La for BP-3 (NS — not sampled).

accompanied by any other metal including those associated with Au mineralization.

Grain size fraction geochemical analyses have also been conducted in the samples from ochre, yellow and purple duricrusts over palaeochannel (BP-1 profile); plus samples from the fragmental and purple duricrusts over the dispersion zone (BF-128 drill hole) and ore zone (BF-159 drill hole) (Fig. 13). The composition of each sample was determined in the <53 μm fraction (matrix) and >0.5 mm fraction (mostly nodules), for direct comparison. The results show that the Au enrichment in the ochre, yellow and upper purple duricrusts over the palaeochannel (BP-1 profile) occurs mostly in the nodules (>0.5 mm) (Fig. 13A) which are distinctly richer in gibbsite, as suggested by the Al_2O_3 enrichment of the >0.5 mm fractions (Fig. 13B) and shown by micromorphological analysis (Fig. 7C). In the residual domain, over ore (BF-159) and dispersion zones (BF-128), Au is not preferentially associated with matrix or nodules.

These results suggest that although the palaeochannel duricrusts tend to be leached in most metals, Au tend to concentrate there especially in

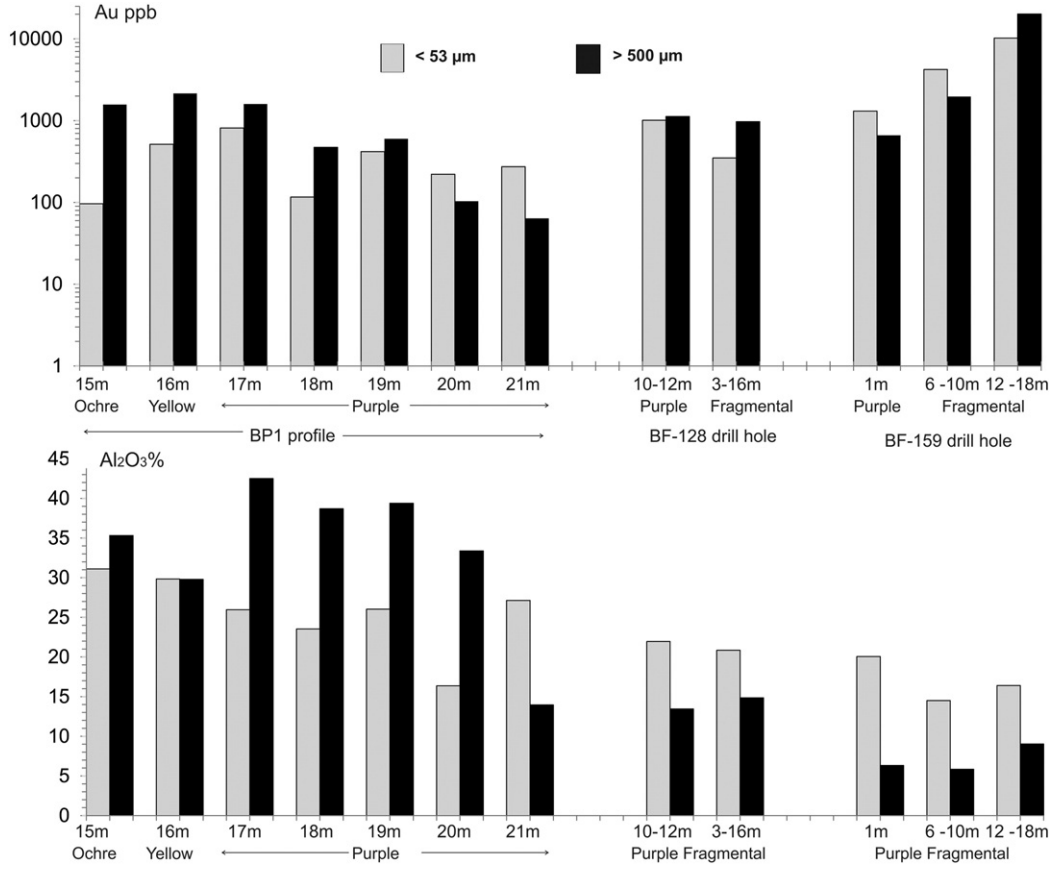

Fig. 13. Gold (A) and Al_2O_3 (B) distributions in fine (<53 μm) and coarse (nodular) fractions of the ferruginous duricrusts over paleo-channel (BP1-profile); dispersion zone (BF1-28 drill hole) and ore zone (BF-159 drill hole).

the upper portions of the duricrusts, preferentially associated with the gibbsitic nodules. It is possible that Au in the palaeochannel duricrusts is chemically precipitated.

11. Geochemistry of latosol components

The geochemistry of the 3 types of nodules plus the fine fraction (<53 μm) of the latosol were investigated in 9 samples: 3 from the BP-1 profile (palaeochannel); 2 from drill hole BF-128 (dispersion zone); and 4 from drill hole BF-165 (close to ore zone). The distribution of Au grades (Fig. 14A) show that the latosol fine fraction is the poorest, while the higher Au grades are always in the concretions in all samples. However, there appears to be no meaningful contrast between the ore zone and palaeochannel or dispersion zone, implying that the nodular fractions of the latosol were widespread. These Au-bearing concretions lack gibbsite and show relicts of saprolite fabric (Fig. 7E). They are probably sourced from the ferruginous duricrust or fragmental duricrust domains originally situated upslope, probably closer to the ore zone, and have been deposited, along with the clay components of the latosol.

Magnetite nodules are the most Fe-rich, and are also the richest in U, Mo, Sn, and W (U shown in Fig. 14B). They are probably derived from magnetic gossan remnants in the ferruginous or fragmental duricrusts. Pisolitic nodules are interpreted as grown in situ within the latosol and have incorporated more mobile metals like Mn (Fig. 14C) and Ag.

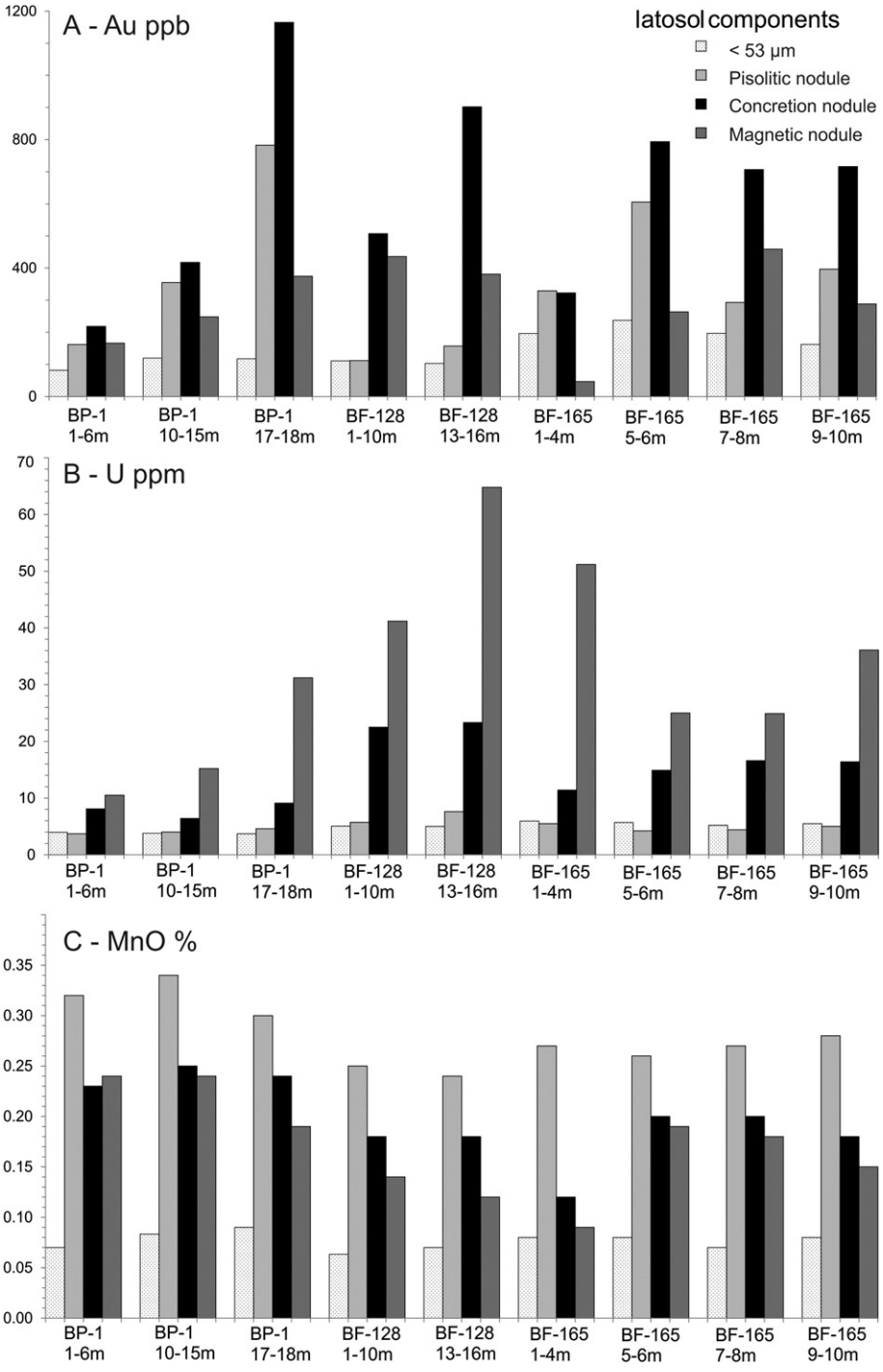

Fig. 14. Distributions of Au (A), U (B) and Mn (C) grades in the latosol components.

12. Distribution of other metals related to mineralization

Concentration data in the regolith over the ore zone and dispersion zone are shown for the most important metals related to Au–Cu mineralization (U, Mo, Pb, Ag, Bi, Sb, Sn, W, P and LREE) in the box-plots of Fig. 15, using the multi-element data base. The data are summarized in Table 1 showing their median grades in the ore and dispersion zones. Despite the relatively low number of samples in each regolith units an attempt is made to broadly describe element behavior. Over the ore zone there is a general leaching tendency in the saprolite, especially if density change is considered. Some metals show an increase in grade due to residual enrichment like W, Pb, Fe and P (shown in Fig. 15A for Pb) or similar grades denoting some leaching like Sn, Sb, Bi and LREE (Fig. 15B and C for Sn and Bi). Metals that are more clearly leached are Mo, U and Ag (Fig. 15D, E, F). In the fragmental duricrust most metals are depleted as a result of gossan leaching, except Au as discussed above, and Fe due to residual concentration followed by U, P, and Sb (Fig. 15E). In the ferruginous duricrust, gossans are further leached, and so are most metals except Sb, Ag, and Bi probably due to their affinity for Fe.

In the dispersion zone, in contrast to the ore zone, there is a general enrichment tendency from protolith to ferruginous duricrust. This difference is related to the mode of occurrence of these metals over the ore zone, where the dominant metal bearing sulfide assemblage is more easily oxidized, generating an acid environment that promotes further leaching (Taylor and Thornber, 1992). In the saprolite Bi, Pb and U are particularly enriched. In the fragmental and ferruginous duricrusts Bi, Ag, and P are also strongly enriched enhancing the dispersion halo around the deposit.

In the latosol most metals are generally depleted and show a more homogeneous distribution.

13. Contrasts and gold correlations

In order to obtain an estimate of the geochemical contrast between the ore and dispersion zones for each metal associated with Au mineralization, the ratio of their median values has been tabulate and added to Table 1 where the Pearson correlation coefficient between Au and these metals are also shown. Most significant contrasts, generally above 5,

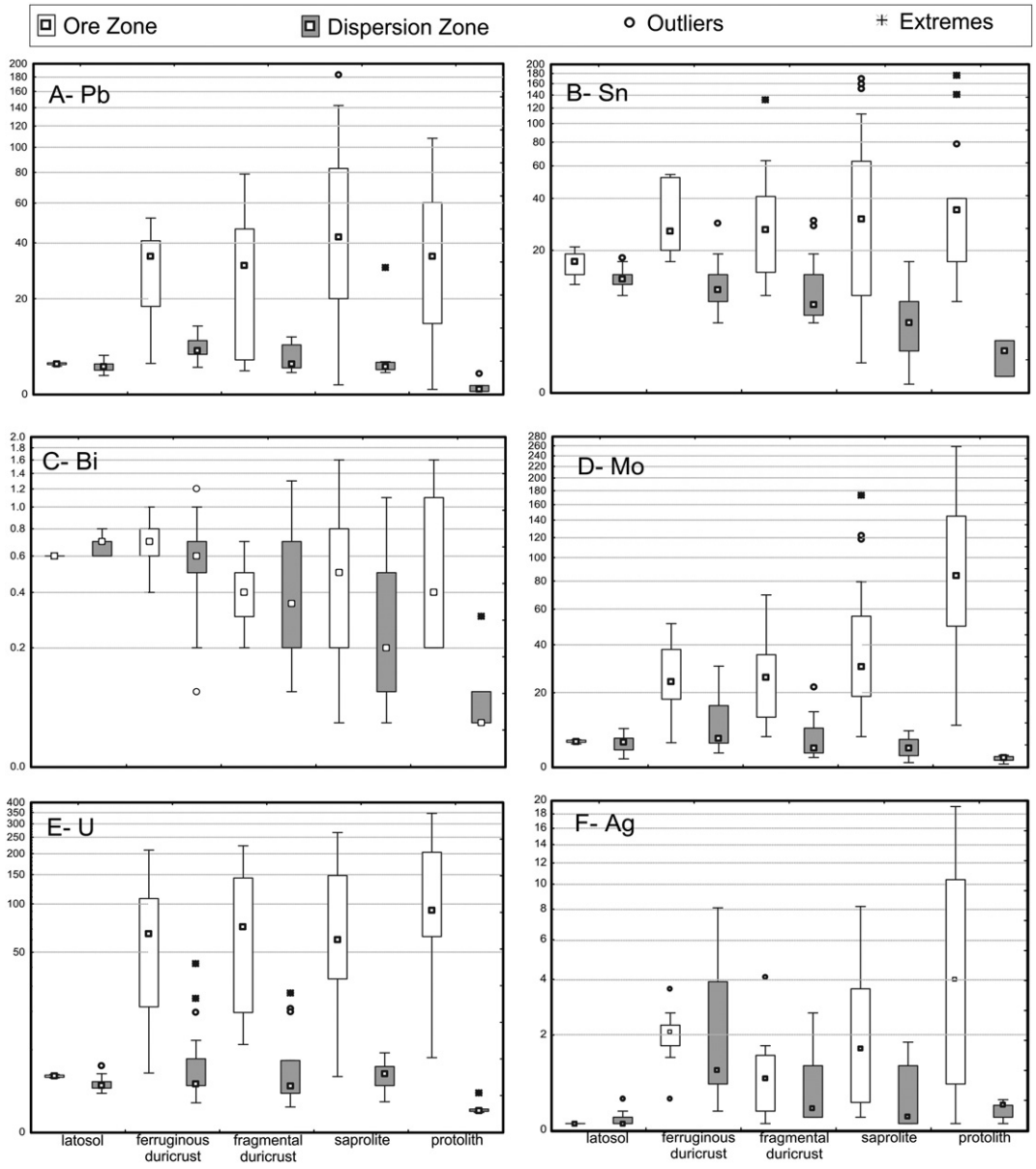

Fig. 15. Box-plots showing the distribution of metals related to Au mineralization in the regolith over the ore zone and dispersion zone. A) Pb; B) Sn; C) Bi; D) Mo; E) U; F) Ag. Number of samples (n) used in the ore zone/dispersion zone: protolith: n = 14/6; saprolite: n = 28/15; fragmental duricrust: n = 12/14; ferruginous duricrust: n = 10/17; latosol n = 5/62.

Table 1
Median grades of Au and associated metals in the ore zone and dispersion zone. The contrasts between the ore zone and dispersion zone for each metal were calculated using the ratio of the median grades. The Pearson correlation coefficients of gold with the other metals are also shown. The background values for duricrust and latosol are taken from the literature mentioned in the text. The ratio between the median metal grades in the dispersion zone and the background values are used to estimate the potential size of the dispersion halo for each metal in six types of sample media. The mean values for each metal and each media are shown in the last column and last row of the Table and these results are also shown in Fig. 16. Significant results reported in the text are marked in bold. Abbreviations: prot = protolith; sap = saprolite; frag = fragmental duricrust; fer = ferruginous duricrust; lat = latosol; lat < 53 μm = latosol fine fraction; pis = pisolitic nodules; conc = concretion nodules; magn = magnetic nodules.

	Median grades in ore zone					Median grades in dispersion zone					Contrast ore × dispersion zones				
	prot	sap	frag	fer	lat	prot	sap	frag	fer	lat	prot	sap	frag	fer	lat
Au ppm	1.08	1.16	3.24	1.34	0.38	0.10	0.11	0.65	0.69	0.17	**10.80**	**10.55**	**4.98**	1.94	2.24
Cu%	0.42	0.15	0.11	0.07	0.01	0.07	0.07	0.04	0.04	0.01	**6.00**	2.02	2.44	1.75	1.00
Bi ppm	0.40	0.50	0.40	0.70	0.60	0.05	0.20	0.35	0.60	0.70	**8.00**	2.50	1.14	1.17	0.86
Ag ppm	4.00	1.60	0.90	2.10	0.10	0.40	0.20	0.35	1.10	0.10	**10.00**	**8.00**	2.57	1.91	1.00
Pb ppm	34.25	45.95	30.85	34.35	4.90	0.75	4.40	4.85	7.40	4.40	**45.67**	**10.44**	**6.36**	4.64	1.11
U ppm	90.95	60.10	72.15	65.40	5.60	1.65	5.90	4.25	4.50	4.30	**55.12**	**10.19**	**16.98**	**14.53**	1.30
Mo ppm	84.40	30.00	25.55	24.00	5.70	1.95	4.10	4.15	6.40	5.55	**43.28**	**7.32**	**6.16**	3.75	1.03
Sn ppm	34.50	30.50	26.50	26.00	17.00	3.00	6.00	8.50	11.00	13.00	**11.50**	**5.08**	3.12	2.36	1.31
∑ LREE	1739.00	1842.00	492.99	320.00	124.61	105.08	120.99	145.05	121.10	118.02	**16.55**	**15.22**	3.40	2.64	1.06
Sb ppm	0.10	0.10	0.10	0.20	0.10	0.05	0.10	0.10	0.20	0.10	2.00	1.00	1.00	1.00	1.00
W ppm	12.20	30.05	16.65	18.85	11.60	4.25	6.60	9.50	9.20	11.80	2.87	4.55	1.75	2.05	0.98
Fe_2O_3%	39.02	50.38	58.50	58.18	33.71	16.33	26.20	42.77	50.74	33.02	2.39	1.92	1.37	1.15	1.02
P_2O_5%	0.25	0.57	0.54	0.57	0.08	0.05	0.04	0.20	0.44	0.11	**5.00**	**14.25**	2.70	1.30	0.73
Mean															

and correlation coefficients, generally above 0.6, are marked in bold in Table 1.

The highest contrasts in the protolith are observed for U, Pb, Mo, LREE, Sn, Au, Ag, Bi, Cu and P, pointing to the relative importance of the enrichment of these metals in the ore zone. Among these metals U, Mo, Sn, and LREE show the strongest correlations with Au. Correlations are also high for Sb and W, but the contrasts are low due to their limited enrichment in the ore zone. The close relation of Au mineralization to monazite (Tallarico et al., 2005) explains the strong contrast and correlations for LREE. However, because P is also present in other types of minerals, its correlation with Au is poor and the associated contrast is low.

In the saprolite the contrasts are generally diminished, but still significant for LREE, P_2O_5, Au, Pb, U, Ag, Mo, and Sn. Correlations with Au remain high for U, Sn, and Mo. Although the contrasts for Au and LREE are high, their correlation coefficient drops from 0.78 to 0.46 showing that Au is dissociated from LREE minerals, including monazite, and its weathering products, although they remain mostly confined to the gossans zones. The increased correlations of Au with Fe_2O_3 and P_2O_5 are due to the occurrence of Au in the gossans, which can also incorporate P in secondary Fe oxides, and P may also remain in other forms of secondary minerals in the gossans causing enrichment and stronger contrast for P_2O_5. The low contrast for Fe is due to widespread ferruginization in the saprolite. Copper leaching is more pronounced in the ore zone compared to the dispersion zone and as a result its contrast diminishes from 6 in the protolith to around 2 in the saprolite and above.

In the fragmental duricrust the contrast is still high for U, Pb, Mo and Au. Gold enrichment is stronger in the dispersion zone compared to the ore zone and this is the cause of its diminished contrast from 10.55 in the saprolite to 4.98 in the fragmental duricrust. High correlations with Au are observed only for Mo, U, and Sn, and reflect the tendency for metal dissociation from Au in the gossans of the fragmental duricrust.

In the ferruginous duricrust contrasts are high only for U, and less so for Pb and Mo. The Au enrichment of the dispersion zone, accompanied by depletion over the ore zone, is the cause of the further diminished Au contrast of the ferruginous duricrust to 1.9. High correlation with Au is observed only for U. In the latosol all Au correlations are lost and contrasts are invariably low.

The general tendency for metal leaching over the ore zone, and enrichment in the dispersion zone, leads to a general decrease in contrast upwards through the regolith and this is followed by a general loss of correlations with Au.

14. Dispersion parameters

To obtain an estimate of the size of the dispersion halos of metals in the ferruginous duricrust and latosol, which are the most important sample media for exploration in lateritic terrains, background values in lateritic profiles were obtained from several locations within the Carajás region (Medeiros Filho, 2003; Horbe, 1995; Araujo, 1994). These background values were taken from samples generally collected over metavolcanic sequences (Table 1). The ratio between the median values of these metals in the ferruginous duricrust and latosol of the dispersion zone, and their background values are taken as an estimate of the potential size of the dispersion halo. Ratios above unity indicate that the grade in the dispersion zone has not yet reached background suggesting that the size of the dispersion halo is potentially larger than ca. 100 m, which is the average distance away from the ore zone that the dispersion zone was sampled in this work.

A similar procedure was adopted to assess the size of the dispersion halo for those metals in the fine fraction of the latosol, and the three types of nodules of the latosol. However, background values for these different types of sample media are not available in the literature. In this case, the background for the latosol fine fraction is the latosol background itself; and the background for the three types of nodules is the ferruginous duricrust background from where these nodules were derived. The results have been added to Table 1 and plotted altogether in Fig. 16 where the mean ratio value for each metal in all six sample media, and the mean ratio value for each sample media for all metals are also shown. Most significant results, generally above 5, are marked bold in Table 1.

The results show that Au has, on average, the largest ratio or dispersion potential, with a mean ratio value of 25.2. The largest values for Au are 44.13 in the concretion nodules followed by 43.12 in the ferruginous duricrust which is an indication that, despite leaching, the lateritic portions of the regolith, including their derived nodules, constitute a good sample media for Au. Gold in the magnetite nodules is not as enriched in relation to background (ratio value near to 18), and probably reflects the dissociation of Au from the magnetic gossan in the ferruginous duricrust. Magnetic nodules carry the geochemical signal of the gossans which are depleted in most metals but still anomalous compared to background values. The pisolitic nodules also show a significant value of 20 which is relatively close to the values obtained for the latosol itself (14.78) or its fine fraction (10.35). Despite the transported nature of the latosol its Au grades have not reached background.

Au correlation coefficient					Backg. values		Ratio median values in the dispersion zone/backg values						
prot	sap	frag	fer	lat	fer	lat	fer	lat	lat < 53 μm	pis	conc	magn	Mean
1.00	1.00	1.00	1.00	1.00	0.016	0.012	**43.12**	**14.78**	**10.35**	**20.56**	**44.13**	**17.94**	25.15
0.33	0.21	0.23	0.12	0.00	0.006	0.003	**6.59**	3.11	1.75	1.95	4.42	3.78	3.60
0.27	0.35	−0.11	−0.06	−0.17	0.500	0.500	1.20	1.40	1.10	**6.40**	**5.40**	**5.20**	3.45
0.42	0.43	0.18	0.19	0.47	0.100	0.100	**11.00**	1.00	1.00	**37.00**	**28.00**	**26.00**	17.33
0.54	0.44	0.50	0.59	0.01	33.875	33.167	0.22	0.13	0.14	0.63	0.40	0.55	0.35
0.74	**0.83**	**0.62**	**0.74**	0.24	2.000	2.000	2.25	2.15	2.53	2.30	**7.45**	**15.60**	5.38
0.87	**0.65**	**0.75**	0.52	−0.08	25.600	14.000	0.25	0.40	0.63	0.67	0.73	1.09	0.63
0.85	**0.76**	**0.62**	0.41	0.10	3.500	3.500	3.14	3.71	**5.52**	3.43	4.29	**8.57**	4.78
0.78	0.46	0.42	0.24	0.00	46.540	53.150	2.60	2.22	2.28	1.71	2.88	4.50	2.70
0.81	0.09	−0.21	−0.12	−0.12	0.200	0.200	1.00	0.50	1.67	3.50	3.50	4.50	2.44
0.79	0.52	0.59	0.45	0.20	5.000	5.000	1.84	2.36	2.11	**37.94**	**5.84**	**42.48**	15.43
0.44	**0.78**	0.39	0.45	0.09	48.089	22.257	1.06	1.48	1.46	1.31	1.35	1.67	1.39
0.49	**0.65**	0.55	0.64	−0.04	0.44	0.12	0.99	0.92	0.67	0.18	0.57	0.45	0.63
							5.52	2.54	2.34	8.47	7.88	9.56	

Considering all metals analyzed, the sample media with the best dispersion potential are the magnetic nodules, where W; Ag; Au; U; Sn and Bi show the highest contrast to background. In the pisolitic nodules W; Ag; Au and Bi are the main metals with high contrast to background, followed by the concretion nodules in which Au shows the highest contrast of all but also includes Ag; U; W and Bi. In the ferruginous duricrust Au; Ag and Cu are the main metals and in the latosol and its fine fraction Au is the only important metal with a high contrast to background.

Generally, Au, Ag, W, U, Sn, Bi, LREE and Sb, are, in that order, the metals that will give the largest dispersion halo, and the best sample media to detect it are in the nodular fraction of the latosol. These are derived from the ferruginous duricrust or fragmental duricrust, but for most metals, the nodule results are better than the ferruginous duricrust. Although the different types of nodules respond differently to each metal, from an exploratory approach, sampling the whole nodule fraction, or lag sampling, seems very acceptable as it is a simple sample media to handle, and will incorporate the most important metals that are indicative to the presence of mineralization.

15. Conclusions

The development of the regolith stratigraphy can be tentatively linked to different weathering regimes through time and related to their geochemical features and efficiency for mineral exploration.

The saprolite and gossan bodies are deeply developed and highly leached in most trace metals associated to Au mineralization, especially Cu, Ag and Mo. The bulk of the Au is also leached but partly concentrated in the gossan ore zones.

Palaeochannels have formed early during regolith evolution. Palaeochannels are not commonly reported in regolith studies conducted in the Carajás region or in lateritic terrains of humid tropical regions. They are more commonly reported in the Western Australia where the lateritic terrains have developed under more arid conditions since at least the Miocene (Butt and Zeegers, 1992; Butt, 1989). At Igarapé Bahia palaeochannels formed by incision of the land surface away from the main outcropping gossan zones. In this irregular relief channels developed and were initially filled with regolith materials eroded

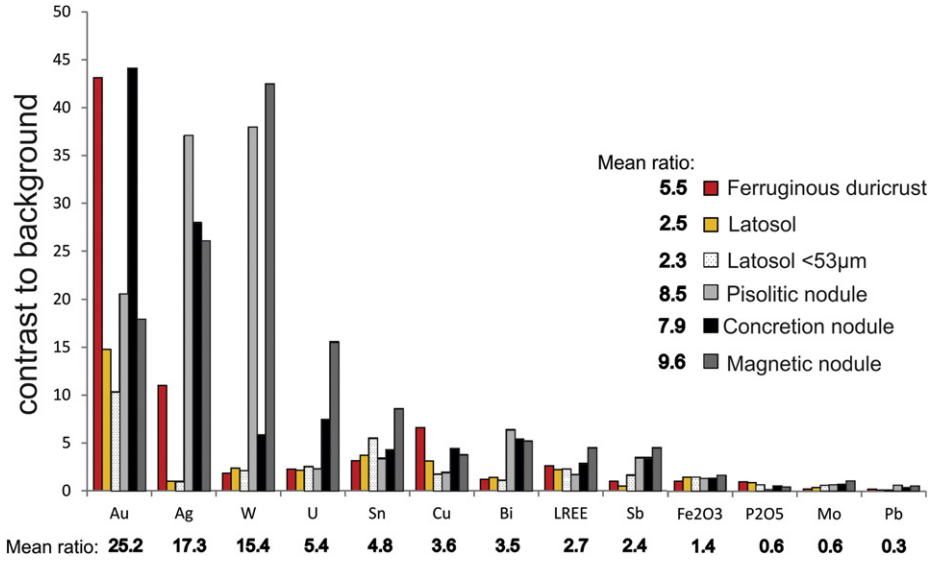

Fig. 16. Potential size of the dispersion halo for gold and related metals in different sample media.

from the upper portions of the saprolite whose original structures were destroyed due to collapsing. Residual Au enrichment probably took place as a result of this collapse. The transported materials accumulated in the lower portions of the channels are poorly sorted and may only locally display sedimentary structures.

As the regolith is further developed the collapsed zones turn into a colluvium. This constitutes the main source of material that accumulates in the channels. The transport mechanism by which colluvium material accumulates into the channels is not clear but it may be a sheet wash type process under semiarid regime (Goudie, 2004). In this way, clay materials and magnetic gossan fragments from upslope are incorporated into the channels. However, colluvium also forms in the residual domains distal to the channel, causing minor lateral dispersion of gossans.

Modification of the morphoclimatic conditions with the development of planation surfaces coupled with the onset of seasonal climatic conditions, promoted intense lateritization of the landscape in the whole Carajás region. At Igarapé Bahia this event has been dated as Eocene (Vasconcelos et al., 1994). Lateritization affects the upper portion of the regolith including the transported materials deposited in palaeochannels. The purple duricrust is formed along with the yellow duricrust on top. Despite planation, the positions of the palaeochannels are marked in the relief as gentle depressions. In fact, lateritization is favored along gentle slopes that facilitate meteoric fluid flow (Butt et al., 2000). The massive duricrusts are formed preferentially on upland positions in response to hardening upon surface exposure (Nahon and Tardy, 1992). During lateritization Au is leached from the ferruginous duricrusts and reprecipitated lower in the fragmental duricrust causing further Au enrichment and lateral dispersion. Work of Andrade et al. (1991) at Igarapé Bahia shows that Au is probably mobilized as organic complexes. Most metals are leached from the ferruginous duricrusts except those that show a greater affinity for Fe like Ag, Bi and Sb.

A further climatic change towards more humid equatorial conditions resulted in the bauxitization of all duricrusts. This phenomenon has been identified elsewhere in the Carajás region by Costa (1997) and Costa et al. (1993). Bauxitization was particularly strong over the palaeochannels where the flow of meteoric fluids was facilitated, forming gibbsitic ferruginous nodules. The transported purple and yellow duricrusts over palaeochannel are best differentiated from the similar duricrusts located over colluvium in the residual domain by their remarkable bauxitic composition. Another effect was the degradation of the upper portions of the ferruginous duricrusts over palaeochannel (Lecomte and Zeegers, 1992). This resulted in the formation of the more friable and gibbsitic ochre duricrust from where most metals are leached, except those that are residually concentrated in resistate minerals (Sn, W, LREE, Ti, and Zr). Gold behavior during bauxitization is difficult to assess with the available data. Although Au shows a similar distribution to the metals that are residually concentrated in the purple, yellow and ochre duricrust samples over palaeochannel, there is also indication that the Au enriched in the gibbistic nodules are chemically transported.

Gold mineralization and bauxitization is also an important feature in the Boddington deposit in Western Australia. Anand (1998) observed that Au is enriched in the bauxite zone below an Au-depleted fragmental and pisolitic duricrust. Gold in the bauxite zone is preferentially concentrated in the fragments not in the matrix. The author suggests that organic acids can dissolve Au from the pisolitic duricrust at surface to precipitate it lower down in the bauxite zone. At Igarapé Bahia solutions impregnated with Au dissolved in organic complexes are more easily channeled through the palaeochannel material where Au is precipitated, however, the chemical mechanisms by which Au precipitates is not clear.

The latest event to complete the regolith profile at Igarapé Bahia is the deposition of a homogeneous latosol layer that fills the remaining depressions left over all palaeochannel sites. This has the effect of flattening the whole landscape over the Carajás laterite surface which is now being eroded by the present drainage network. The latosol is extremely depleted in all metals as it incorporates barren materials from paleo upslope positions. But it also incorporates metal bearing ferruginous nodules derived from the erosion of duricrusts located closer to mineralization.

The problem geochemical exploration faces in lateritic terrains dominated by transported cover has been extensively addressed in Western Australia where exploration effectiveness has been improved by using alternative sample media (Anand and Paine, 2002; Matthias et al., 2001) or by understanding mechanisms of metal transfer through cover aiming to refine analytical methods (Anand et al., 2014; Anand et al., 2007; Mann et al., 2005; Aspandiar et al., 2004).

To improve geochemical exploration effectiveness in the regolith dominated terrain of the Carajás region, the origin and nature of the regolith materials available for sampling must be appreciated. From the work conducted here it becomes clear that routine soil sampling generally adopted in exploration campaigns may be misleading if applied in the Carajás region due to the transported nature of the latosol.

The ferruginous duricrusts may constitute an alternative sample media but they are not always available at surface for sampling or they may be transported in the vicinities of palaeochannels. Ferruginous duricrusts near palaeochannels tend to be more leached in most metals compared to similar ferruginous duricrusts over colluvium in residual domains. On the contrary, Au may be enriched in the gibbsitic ferruginous duricrusts over palaeochannel. It is therefore important to identify the environment in which ferruginous duricrusts are formed since this can greatly affect geochemical exploration parameters such as threshold and background values. Identification of palaeochannel sites from surface is an important topic for further research.

Despite the considerations outlined above, the attempt to estimate the dispersion potential of the main metals associated to Au mineralization using different types of sample media indicated that the nodular fractions of the latosol show the best results as they include a larger suit of metals with high dispersion potential including Au, Ag, W, U, Bi and Sn. The results for the ferruginous duricrust are also satisfactory for Au, Ag and Cu. This shows that lag sampling at surface is a promising procedure to detect anomalous signals from mineralization at depth. However, due to the widespread dispersion of the nodules in the latosol, follow up surveys are necessary to better locate the source of the anomalies. The effectiveness of lag sampling has never been reported in the lateritic terrain of the Amazon region where the nature of the regolith materials and regolith evolution need to be more deeply studied.

Conflict of interest

I do not have suggestions of potential reviewers with conflict of interest.

Acknowledgments

The results presented here are based on the work conducted as part of the LATAM Project aimed to study the regolith over mineral deposits in the Amazon. This project included several earth scientists from the Federal University of Rio de Janeiro, Federal University of Pará, University of São Paulo, Campinas University and Geological Survey of Brasil (CPRM) whose efforts are greatly acknowledged. The financial assistance received from the CT-Mineral/CNPq/MCT (proc. 506292/2003-7) is greatly acknowledged. Vale Ltd. is acknowledged for providing support for field work and letting access to the exploration data base and core samples at Igarapé Bahia mine. The Centre for Mineral Technology (CETEM) of CNPq is thanked for helping with the SEM analysis. The author wishes to thank the contributions received from the reviewers and the encouragement received from Dr. Ignacio González-Álvarez from the Mineral Resources and Regolith Team Research Groups of CSIRO to present this paper. Dr. Eric Hiatt is thanked for reviewing the manuscript and Dr. Ana Dreher for clarifications on the bedrock geology of the region.

Appendix A. Whole geochemical results of ten representative samples

Regolith unit	Protolith ore	Ferruginous saprolite	Fragmental duricrust	Purple duricrust	Yellow duricrust	Massive duricrust	Ochre duricrust	Latosol layer	Ferruginous sediment	Concretion nodule
Sample	BAH-04	BF159-20	BP2-4	BP-11-3	BP-11-2	BP-11-1	BP3-11	BP3-26	BP3-6	BP1-10
SiO_2 %	33.48	29.48	8.88	4.42	10.29	12.82	4.87	15.52	11.7	13.8
Al_2O_3 %	7.06	25.61	30.37	20.94	17.58	16.32	38.83	29.02	17.77	14.21
Fe_2O_3 %	39.17	28.48	41.93	56.16	57.66	58.85	32.03	34.93	59.97	61.22
MgO %	2.61	0.03	0.04	0.37	0.37	0.04	0.05	0.06	0.02	0.08
CaO %	8.25	0.01	0.01	0.06	0.06	0.01	0.01	0.01	0.02	0.03
Na_2O %	0.83	0.01	0.02	0.07	0.07	0.02	0.02	0.02	0.02	0.04
K_2O %	0.7	0.05	0.04	<0.04	<0.04	<0.04	0.04	0.04	0.04	<0.04
TiO_2 %	0.26	1.95	1.74	1.94	2.35	1.36	2.44	2.55	1.18	1.46
P_2O_5 %	1.15	0.43	0.13	0.18	0.14	0.09	0.08	0.11	0.15	0.13
MnO %	0.63	0.37	0.1	0.39	0.25	0.1	0.06	0.05	0.06	0.25
Cr_2O_3 %	0.01	0.04	0.032	0.015	0.035	0.039	0.04	0.04	0.032	0.392
LOI %	4.2	13.1	16.6	15.2	11.1	10.2	21.4	17.6	8.9	8.2
TOT/C %	0.81	0.12	0.08	0.09	0.08	0.08	0.14	0.9	0.06	0.1
TOT/S %	1.09	0.05	0.04	0.01	0.04	0.05	0.04	0.07	0.02	<0.01
SUM %	98.37	99.57	99.86	99.8	99.97	99.91	99.85	99.93	99.84	99.83
Ba ppm	96.1	99.6	5	17.9	4	5.7	12.6	17.2	16.6	4.9
Be ppm	1	2	<1	1	1	<1	<1	<1	<1	<1
Co ppm	77.6	17.1	2.2	12.3	6.8	2.6	2	4.4	10.2	13.5
Cs ppm	1.1	0.05	<0.1	<0.1	<0.1	<0.1	<0.1	<0.1	<0.1	<0.1
Ga ppm	10.7	27.5	30.1	29.3	27	32.3	46.4	48.3	35.8	35.7
Hf ppm	0.9	4.7	5.1	5.2	6.2	5.2	12.1	14.5	7	8
Nb ppm	4.6	8.1	9.9	8.8	11.4	10.4	25.3	27.9	13.7	12.4
Rb ppm	17.6	1.5	<0.5	<0.5	<0.5	<0.5	<0.5	0.7	0.5	<0.5
Sc ppm	13	58	24	36	34	35	26	26	24	37
Sn ppm	13	5	6	11	7	10	12	16	30	11
Sr ppm	54.4	6.2	7.7	12.1	7.2	6.1	13.6	15.1	12.2	6.1
Ta ppm	0.2	0.7	0.7	0.2	0.3	0.3	1.9	2.4	1	0.7
Th ppm	3.3	4.4	9.7	9.7	11.1	11.8	28.4	29	22.9	40.5
U ppm	177.9	18.7	2	4.4	3.8	4	4	7.1	20.9	6.4
V ppm	100	321	362	314	497	521	359	348	499	511
W ppm	0.9	13.4	7.6	4.5	7.9	6.5	10.1	12.2	22.1	24.8
Zr ppm	39	152.5	168.8	187.5	217.7	180.2	410.8	467.7	232.6	269.3
Y ppm	63.6	28.2	12.8	31.6	16.4	14.2	22.8	25.9	22.2	15
La ppm	707.9	49	35.8	43.6	18.6	48.7	68.3	62.7	96.9	26.5
Ce ppm	1158	109.8	32.3	53	17.3	48.1	59.7	93.3	123.7	41.4
Pr ppm	96.65	7.33	3.93	5.43	2.19	5.36	7.48	6.36	8.95	2.91
Nd ppm	272.4	23.4	10.5	15.2	5.9	13.9	19.9	17.1	19.7	7.7
Sm ppm	29.58	4	1.4	2.6	0.98	1.53	2.4	2.3	2.1	1.2
Eu ppm	10.17	1.53	0.43	1.27	0.44	0.52	0.87	0.92	0.83	0.47
Gd ppm	17.07	3.89	1.31	3.17	1.25	1.28	2.11	2.32	1.72	1.54
∑LREE	2291.77	198.95	85.67	124.27	46.66	119.39	160.76	185	253.9	81.72
Tb ppm	2.84	0.83	0.27	0.79	0.35	0.34	0.47	0.54	0.46	0.39
Dy ppm	12.55	5.02	1.91	4.43	2.16	1.82	3.05	3.67	3.18	2.23
Ho ppm	2.23	1.09	0.47	0.96	0.51	0.41	0.8	0.89	0.8	0.48
Er ppm	6.05	3.21	1.48	2.84	1.59	1.26	2.45	2.87	2.75	1.73
Tm ppm	0.81	0.5	0.23	0.42	0.28	0.19	0.38	0.45	0.44	0.25
Yb ppm	4.75	3.36	1.69	2.82	1.93	1.36	2.46	2.97	2.42	1.54
Lu ppm	0.69	0.5	0.27	0.45	0.32	0.24	0.38	0.43	0.42	0.25
Mo ppm	96.8	9.6	3	4.9	5.9	11	2.1	6.5	9.1	11.6
Cu ppm	>10000	1757.4	233.4	812.3	431.9	81.9	45.9	143.5	125.4	176
Pb ppm	60.3	1.5	4.2	4.5	4.9	8.4	2.2	4.9	6.9	15.6
Zn ppm	28	18	9	36	16	3	4	11	6	11
Ni ppm	84.3	24.6	3.1	9.3	7.4	2	2	15	16.5	6.5
As ppm	30.7	0.8	0.7	5.4	7.3	8.9	<,5	3.5	10.7	16.1
Cd ppm	<0.1	0.05	<0.1	<0.1	<0.1	<0.1	0.1	0.1	<0.1	<0.1
Sb ppm	0.1	0.05	0.1	0.1	0.1	0.3	0.1	0.1	0.2	0.8
Bi ppm	4.9	0.2	0.2	0.2	0.2	0.4	0.6	0.6	0.6	3.5
Ag ppm	10.4	0.3	1.2	1.4	3.2	1.8	0.4	0.1	0.2	2.6
Hg ppm	<0.1	0.02	0.28	0.08	0.19	0.05	0.29	0.11	0.02	1.26
Tl ppm	0.1	0.05	<0.1	<0.1	<0.1	<0.1	<0.1	<0.1	<0.1	<0.1
Se ppm	3.6	0.7	<0.5	<0.5	<0.5	<0.5	<0.5	<0.5	<0.5	0.7
Au ppb	4292.5	641.6	363.8	146.1	194.2	390.2	457	55.8	53.8	417.7

References

Almada, M.C.O., Villas, R.N., 1999. O Depósito Bahia: exemplo de depósito arqueano vulcanogênico de sulfetos de Cu ± Au tipo Bessi em Carajás, Pará. SBG, Simpósio de Geologia da Amazônia, 6, Manaus, Boletim de Resumos Expandidos, pp. 98–101.

Anand, R.R., 1998. Regolith-landform evolution and geochemical dispersion from the Boddington gold deposit, Western Australia. Open File Report 3, CRC LEME CSIRO Perth, Australia. CSIRO, Division of Exploration.

Anand, R.R., 2001. Evolution, classification and use of ferruginous regolith materials in exploration, Yilgarn craton. Geochem. Explor. Environ. Anal. 1, 221–236.

Anand, R.R., Butt, C.R.M., 2010. A guide for mineral exploration through the regolith in the Yilgarn craton. Aust. J. Earth Sci. 57, 1015–1114.

Anand, R.R., Paine, M., 2002. Regolith geology of the Yilgarn Craton, Western Australian — implication for exploration. Aust. J. Earth Sci. 49 (1), 3–163.

Anand, R.R., Verrall, M., 2011. Biological origin of minerals in pisoliths in the Darling Range of Western Australia. Aust. J. Earth Sci. 58 (7), 823–833.

Anand, R.R., Cornelius, M., Phang, C., 2007. Use of vegetation and soil in mineral exploration in areas of transported overburden, Yilgarn craton, Western Australia. Geochem. Explor. Environ. Anal. 7, 267–288.

Anand, R., Lintern, M., Noble, R., Aspandiar, M., Macfarlane, C., Hough, R., Stewart, A., Wakelin, S., Townley, B., Reid, N., 2014. Geochemical dispersion through transported cover in regolith-dominated terrains—toward an understanding of process Chapter 6 Econ. Geol. Spec. Publ. 18, 97–125.
Andrade, W.O., Machesky, M.L., Rose, A.W., 1991. Gold distribution and mobility in the surficial environment, Carajas region, Brazil. J. Geochem. Explor. 40, 95–114.
Araujo, E.S. 1994. Geoquímica multi-elementar de crostas e solos lateríticos da Amazônia Oriental. Universidade Federaldo Pará, Instituto de Geociências, Unpublished DSc Thesis 360 pp.
Aspandiar, M.F., Anand, R.R., Gray, D., Cucuzza, J., 2004. Mechanisms of metal transfer through transported overburden within the Australian regolith. Explore 125, 9–12.
Barros, C.E.M., Macambira, M.J.B., Barbey, P., Scheller, T., 2004. Dados isotópicos Pb–Pb zircão (evaporação) e Sm_nd do Complexo Granítico Estrela, Província Mineral do Carajás, Brasil: Implicações petrológicas e tctônicas. Rev. Bras. Geosci. 34531–34538.
Beauvais, A., Tardy, Y., 1993. Degradation and dismantling of iron crust under climatic changes in central Africa. Chem. Geol. 107, 277–288.
Boulangé, B., Carvalho, A., Carvalho, A., Boulangé, B., 1997. The bauxite of Porto Trombetas. In: Melfi, A.J., Lucas, Y. (Eds.), Brazilian Bauxites. USP/FAPESP/ORSTOM, Brazil, pp. 55–73.
Butt, C.R.M., 1989. Genesis of supergene gold deposits in the lateritic regolith of the Yilgarn block, Western Australia. Econ. Geol. Monogr. 6, 460–470.
Butt, C.R.M., Zeegers, H., 1992. Regolith Exploration Geochemistry in Tropical and Sub-tropical Terrains. In: Govett (Ed.)Handbook of Exploration Geochemistry 4. Elsevier Science Publishers B.V., Amsterdam (607 pp.).
Butt, C.R.M., Lintern, M., Anand, R.R., 2000. Evolution of regoliths and landscapes in deeply weathered terrain — implications for geochemical exploration. Ore Geol. Rev. 16, 167–183.
Cornelius, M., Smith, R.E., Cox, A.J., 2001. Laterite geochemistry for regional exploration surveys — a review, and sampling strategies. Geochem. Explor. Environ. Anal. 1, 211–220.
Corrêa Neto, T.A., 2009. Estudo de Perfis Lateríticos na Mina do Igarapé Bahia, Carajás. Universidade Federal do Rio de Janeiro, Departamento de Geologia (PhD Thesis, 278 pp.).
Costa, M.L., 1997. Lateritization as a major process of ore deposit formation in the Amazon region. Explor. Min. Geol. 6 (1), 79–104.
Costa, M.L., Vieira-Costa, J.A., Angélica, R.S., 1993. Gold-bearing bauxitic laterite in a tropical rain forest climate: Cassipore, Amapá, Brazil. Chron. Rech. Min. 510, 41–52.
Costa, M.L., Angélica, R.S., Fonseca, L.R., 1996. Geochemical exploration for gold in deep weathered lateritized gossans in the Amazon Region, Brazil: a case history of the Igarapé Bahia deposit. Geochim. Bras. 10 (1), 13–26.
Docegeo, 1988. Revisão litoestratigráfica da Província Mineral de Carajás. SBG, Congresso Brasileiro de Geologia, 35, Belém, Anexo aos Anais, pp. 11–54.
Dreher, A.M., Xavier, R.P., Martini, S.L., 2005. Fragmental rocks of the Igarapé Bahia Cu–Au deposit, Carajás Mineral Province, Brazil. Rev. Bras. Geogr. 35, 358–368.
Dreher, A.M., Xavier, R.P., Taylor, B.E., Martini, S.L., 2008. New geologic, fluid inclusion and stable isotope studies on the controversial Igarapé Bahia Cu–Au deposit, Carajás Province, Brazil. Mineral. Deposita 43, 161–184.
Eggleton, R.A. 2001. The Regolith Glossary, Surficial Geology, Soils and Landscapes (Ed.) CRC LEME Pub. 144 pp.
Freyssinet, P., 1993. Gold dispersion related to ferricrete pedogenesis in south Mali: application to geochemical exploration. Chron. Rech. Min. 510, 24–40.
Goudie, A.S. (Ed.)2004. Encyclopedia of Geomorphology 1. Routledge (1156 pp.).
Grubb, P.L.C., 1979. Genesis of bauxite deposits in the lower Amazon Basin and Guianas coastal plain. Econ. Geol. 74, 735–750.
Hieronymus, B., Bildgen, P., Kotschoubey, B., Boulangé, A.M., Kensabiec, A.M., 1989. Comparative study of three bauxitic process. Int. Congr. ICSOBA 6 (22), 115–125.
Horbe, A.M.C. 1995. Evolução mineralógica e geoquímica multi-elementar de perfis de solos sobre lateritos e gossans na Amazônia. Universidade Federal do Pará, Instituto de Geociências, Unpublished PhD Thesis 213p.
Horbe, A.M.C., Costa, M.L., 2005. Lateritic crusts and related soils in eastern Brazilian Amazonia. Geoderma 126, 225–239.
Ker, J.C., 1997. Latossolos do Brasil: Uma Revisão. Rev. Geonomos 5 (1), 17–40.
Kronberg, B.I., Fife, W.S., Mckinnon, B.J., Couston, J.F., Stilianidi Filho, B., Nash, R.A., 1982. Model for bauxite formation: Paragominas, Brazil. Chem. Geol. 35, 311–320.
Lecomte, P., Zeegers, H., 1992. Humid tropical terrains (rainforests). In: Butt, C.R.M., Zeegers, H. (Eds.), Regolith Exploration Geochemistry in Tropical and Subtropical TerrainsHandbook of Exploration Geochemistry vol. 4. Elsevier, Amsterdam, pp. 41–55.
Leprun, J.C., 1979. Les cuirasses ferrugineuses des pays cristallins de l'Afrique Occidentale se'che. Gene'se-transformations-de'gradation. Sci. Geol. Mem. 58, 1–223.
Lucas, Y., Kolbisek, B., Chauvel, A., 1989. Structure, genesis and present evolution of Amazonian bauxites developed on sediments. Intern. Congr. ICSOBA 6, Poços de Caldas, 1989 vol. 22. Anais, Poços de Caldas, Brazil, pp. 81–94.
Mann, A.W., Birrell, R.D., Fedikow, M.A.F., de Souza, H.A.F., 2005. Vertical ionic migration: Mechanisms, soil anomalies, and sampling depth for mineral exploration. Geochem. Explor. Environ. Anal. 5, 201–210.
Matthias, C., Smith, R.E., Cox, A., 2001. Laterite geochemistry for regional exploration surveys—a review, and sampling strategies. Geochem. Explor. Environ. Anal. 1, 211–220.
Medeiros Filho, C.A. 2003. Prospecção Geoquímica e Mapeamento de Regolito na Região de Carajás, Estado do Pará. Universidade Federal do Pará, Instituto de Geociências, Unpublished MSc dissertation, 140p.
Nahon, D., Tardy, Y., 1992. The ferruginous laterites. In: Butt, C.R.M., Zeegers, H. (Eds.), Regolith Exploration Geochemistry in Tropical and Subtropical TerrainsHandbook of Exploration Geochemistry 4. Elsevier, Amsterdam, pp. 41–55.
Nogueira, A.C.R., Truckenbrodt, W., Costa, J.B.S., Pinnheiro, R.V.L., 1994. Análise faciológica e estrutural da Formação Águas Claras, Pré-cambriano da Serra dos Carajás. SBG, Simpósio Geologia Amazônia, 4, Belém, Boletim de Resumos Expandidos, pp. 363–364.
Porto, C.G., 2007. Caracterização do regolito para a exploração mineral em terrenos lateríticos na Amazônia — Projeto Latam. Relatório final de pesquisa, CNPq proc. 506292/2003–7. Dep. Geologia, Instituto de Geociências, UFRJ (318 pp.).
Sombroek, W.G., 1966. Amazon soils. A reconnaissance of the soils of the Brazilian Amazon Region. Centre Agric. Publ., Wageningen (292 pp.).
Tallarico, F.H.B., Oliveira, C.G., Figueiredo, B.R., 2000. The Igarapé Bahia primary Cu–Au mineralization, Carajás Province: a descriptive model and genetic considerations. Rev. Bras. Geoci. Bras. 30 (2), 230–233.
Tallarico, F.H.B., McNaughton, N.J., Groves, D.I., Fletcher, I.R., Figueiredo, B.R., Carvalho, J.B., Rego, J.L., Nunes, A.R., 2004. Geology and Shrimp II U–Pb constraints on the age and origin of the Breves Cu–Au–(W–Bi–Sn) deposit, Carajás, Brazil. Mineral. Deposita 39, 68–86.
Tallarico, F.H.B., Figueiredo, B.R., Groves, D.I., Kositcin, N., McNaughton, N.J., Fletcher, I.R., Rego, J.L., 2005. Geology and Shrimp U–Pb geochronology of the Igarapé Bahia deposit, Carajás copper–gold belt, Brasil: an Archean (2.57 Ga) example of iron-oxide Cu–Au(U–REE) mineralization. Econ. Geol. 100, 7–28.
Tavaza, E., Oliveira, C.G., 2000. The Igarapé Bahia Au–Cu (REE–U) deposit, Carajás, Brazil. In: Porter, T.M. (Ed.), Hydrotemal Iron Oxide Copper–Gold & Related Deposits: A Global Perspective. Australian Mineral Foundation, Adelaide, pp. 203–212.
Taylor, G.F., Thornber, M.R., 1992. Gossan formation and gossan surveys: introduction. In: Butt, C.R.M., Zeegers, H. (Eds.), Regolith Exploration Geochemistry in Tropical and Subtropical TerrainsHandbook of Exploration Geochemistry 4. Elsevier, Amsterdam (607 pp.).
Thorne, R., Anand, R.R., Suvorova, A., 2014. The formation of fluvio-lacustrine ferruginous pisoliths in the extensive palaeochannels of the Yilgarn Craton, Western Australia. Sediment. Geol. 313, 32–44.
Truckenbrodt, W., Kotschoubey, B., 1981. Argila de Belterra–Cobertura terciária das bauxitas amazônicas. Rev. Bras. Geol. 11, 203–208.
Vasconcelos, P.M., Becker, T.A., Renne, P.R., Brimhall, G.H., 1994. Direct dating of weathering phenomena by K–Ar and $^{40}Ar/^{39}Ar$ analysis of supergene-Mn oxides. Geochim. Cosmochim. Acta 58, 1635–1665.